



Sensitivity analysis via Karhunen-Loève expansion of a random field model: estimation of Sobol' indices and experimental design

Luc Pronzato

► To cite this version:

Luc Pronzato. Sensitivity analysis via Karhunen-Loève expansion of a random field model: estimation of Sobol' indices and experimental design. Reliability Engineering and System Safety, 2019, 187, pp.93-109. 10.1016/j.ress.2018.01.010 . hal-01545604v2

HAL Id: hal-01545604

<https://hal.science/hal-01545604v2>

Submitted on 11 Jan 2018

HAL is a multi-disciplinary open access archive for the deposit and dissemination of scientific research documents, whether they are published or not. The documents may come from teaching and research institutions in France or abroad, or from public or private research centers.

L'archive ouverte pluridisciplinaire **HAL**, est destinée au dépôt et à la diffusion de documents scientifiques de niveau recherche, publiés ou non, émanant des établissements d'enseignement et de recherche français ou étrangers, des laboratoires publics ou privés.

Sensitivity analysis via Karhunen-Loève expansion of a random field model: estimation of Sobol’ indices and experimental design

Luc PRONZATO^{*†}

January 11, 2018

Abstract

We use the Karhunen-Loève expansion of a random-field model to construct a tensorised Bayesian linear model from which Sobol’ sensitivity indices can be estimated straightforwardly. The method combines the advantages of models built from families of orthonormal functions, which facilitate computations, and Gaussian-process models, which offer a lot of flexibility. The posterior distribution of the indices can be derived, and its normal approximation can be used to design experiments especially adapted to their estimation. Implementation details are provided, and values of tuning parameters are indicated that yield precise estimation from a small number of function evaluations. Several illustrative examples are included that show the good performance of the method, in particular in comparison with estimation based on polynomial chaos expansion.

Keywords: sensitivity analysis, Sobol’ indices, random-field model, Karhunen-Loève expansion, Bayesian linear model, polynomial chaos, optimal design of experiments.

1 Introduction and problem statement

We consider global sensitivity analysis for a function $f(\cdot)$ depending on d real input variables $\mathbf{x} = (x_1, \dots, x_d)$. Uncertainty on the inputs is accounted for by treating them as random variables. We shall denote $\mathbf{X} = (X_1, \dots, X_d)$ the corresponding random vector, the probability measure μ of which is supposed to have the tensor-product form

$$d\mu(\mathbf{x}) = d\mu_1(x_1) \times \dots \times d\mu_d(x_d), \quad (1.1)$$

with μ_i a probability measure over $\mathcal{X}_i \subseteq \mathbb{R}$, $i = 1, \dots, d$. Global sensitivity analysis aims at identifying important variables, and possibly important interactions between groups of variables, in the sense that they are the most influential on the global behaviour of $f(\cdot)$ with respect to μ . The calculation of Sobol’ indices, which quantify the portion of the variance of $f(\mathbf{X})$ explained by each input, or combination of different inputs, see Section 2.1, has become a standard tool in sensitivity analysis for measuring the importance of (groups of) variables; see in particular the recent overview [26].

Commonly used estimation methods of Sobol’ indices include the Fourier Amplitude Sensitivity Test (FAST) [6, 32, 7], see also [31]; the model-free pick-and-freeze methods [33, 30] based on QMC sampling designs, Latin hypercubes (Lh) or orthogonal arrays, see in particular [22, 36, 15, 16].

^{*}Luc.Pronzato@cirs.fr (corresponding author)

[†]Université Côte d’Azur, CNRS, I3S, France

In case of functions $f(\cdot)$ of computationally expensive evaluation, the use of metamodels, possibly combined with Monte-Carlo sampling, allows estimation of indices from a reduced number of data points; see e.g., [25, 23, 20]. The calculation of Sobol' indices is then considerably facilitated when the metamodel used has a particular form, which is especially adapted to the underlying Sobol'-Hoeffding decomposition.

(i) Polynomial Chaos Expansions (PCE) correspond to tensor products of univariate polynomial models $P_i(x_i)$, each $P_i(\cdot)$ belonging to a family of orthogonal polynomials with respect to μ_i , and provide an easy evaluation of Sobol' indices. Indeed, the indices are given by ratios of quadratic forms in estimated parameters for the linear regression model defined by the PCE; see [35, 3, 1]. The precision of the estimated indices can be related to the information matrix for the linear regression model, which allows the construction of efficient designs adapted to the estimation of Sobol' indices; see [5]. Families of orthogonal polynomials are known for particular distributions (e.g., Hermite for the standard normal, Legendre for the uniform distribution, etc.), but transformations or calculation via moment matrices can be used in more general situations, see Section 4.1.

(ii) To a given Random-Field (RF) model with tensor-product covariance (see [34, p. 54]) and a tensorised probability measure μ , one can associate a particular ANOVA kernel that yields a simple expression for the Sobol' indices, see [9]. The construction of the ANOVA kernel is explicit for some particular RF covariances and measures μ only, but numerical integration can be used otherwise. See also [17] for the ANOVA decomposition of a kernel, with some insights into the consequence of enforcing sparsity through the choice of a sparse kernel.

On the other hand, both approaches suffer from some limitations. The number of monomials to be considered in a PCE model grows very fast with the number d of variables, so that many observations (function evaluations) are required to get an estimate of the indices, even for moderate values of d . Moreover, the polynomial model seems to offer less flexibility than a RF model with covariance chosen in a suitable family (for instance the Matérn class, see [34, Chap. 2]) that specifies the regularity of the RF realisations (i.e., of the function to be approximated). In the approach based on ANOVA kernels, no simple characterisation of the precision of the estimation, which could be used for experimental design, is available (see [17, Remark 5]). Moreover, no simple recursive calculation of the indices seems possible in the case where data are collected successively.

The objective of the paper is to present a method that combines the positive aspects of (i) and (ii): starting with an arbitrary Gaussian RF model with covariance in the tensor-product form, following the approach in [14], we construct a Bayesian Linear Model (BLM) through a particular Karhunen-Loève expansion of the field associated with the tensor-product measure μ ; see also [12]. Like in a PCE model, the regression functions of variable i are orthogonal for μ_i , $i = 1, \dots, d$ (they may possibly also include a few polynomial terms), but in addition to a PCE model the parameters have here a particular joint prior normal distribution, with diagonal covariance governed by the covariance function of the RF. The Sobol' indices (*of any order*) are obtained straightforwardly from the estimated parameters in the BLM, and the presence of a prior allows estimation from a few observations only. Like in [5], the linearity of the model facilitates the recursive estimation of the indices in case of sequential data collection. The sequential selection of observation points (sequential design) ensuring a precise estimation of the indices can easily be implemented, and various selection rules can be considered depending on which characterisation of precision is preferred. Approximate design theory can also be used to construct an optimal design measure for the estimation of Sobol' indices through the solution of a convex problem, from which an exact design (without repetitions of observations) can be extracted.

The computation of Sobol' indices via the Karhunen-Loève expansion of a covariance operator is also considered in [13], but in a different framework. The authors consider an additive model with functional inputs and, using properties of U-statistics, they investigate the asymptotic properties of

an estimator of first-order indices when the truncation level N of the expansion grows at suitable rate as a function of the number n of observations. The situation is much different in the present paper: we consider a general nonlinear function $\mathbf{f}(\cdot)$ of scalar inputs and our Karhunen-Loève expansion concerns a random-field model of $\mathbf{f}(\cdot)$. The number N of regression functions in the obtained BLM and the regression functions themselves are fixed, with N of the same order of magnitude as the number n of observations. We shall not investigate the asymptotic properties of our estimator of Sobol' indices as N and n tend to infinity. For fixed N , i.e., for a fixed BLM, the estimated indices tend to the true indices of that BLM as n tends to infinity and satisfy a central limit theorem (under standard assumptions concerning Bayesian estimation in a linear regression model). However, since N is fixed, the estimated indices do not converge to the true indices of $\mathbf{f}(\cdot)$ as n tends to infinity. Note that we are mainly interested in the case where n is small, a prerequisite when $\mathbf{f}(\cdot)$ is expensive to evaluate, and we are more concerned with the choice of the n design points ensuring a precise estimation of the indices than with asymptotic properties for large n , when $N = N(n)$ grows with n at suitable rate.

Section 2 gives a brief overview of the Sobol'-Hoeffding decomposition and the estimation of Sobol' indices in models given by tensor products of orthonormal functions. The tensorised BLM is introduced in Section 3 for a product measure μ . Its practical implementation relies on finitely supported measures, typically quadrature approximations, and is detailed in Section 4 with some numerical illustrations. Section 5 considers the estimation of Sobol' indices in the BLM, together with the construction of posterior distributions and credible intervals. In Section 6, the normal approximation of the posterior distribution is used to design experiments adapted to the estimation of Sobol' indices. The examples in Section 7 illustrate the performance of the method, in particular in comparison with PCE. The construction of optimal (non-adaptive) designs is considered in an Appendix.

2 Sobol' sensitivity indices

2.1 The Sobol'-Hoeffding decomposition and Sobol' indices

Let $f(\cdot)$ be a function depending on d input variables $\mathbf{x} = (x_1, \dots, x_d) \in \mathcal{X} \subseteq \mathbb{R}^d$ and μ denote a probability measure on \mathcal{X} . We assume that μ has the tensor-product form (1.1) and that $f(\cdot)$ is square integrable for μ , which we shall abusively denote by $f \in L^2(\mathcal{X}, \mu)$, with $L^2(\mathcal{X}, \mu)$ the Hilbert space of real-valued functions on \mathcal{X} square integrable for μ . (Note that elements of $L^2(\mathcal{X}, \mu)$ are in fact equivalence classes of functions that coincide μ -almost everywhere.) We denote by $\mathbf{E}_\mu\{\cdot\}$ and $\text{var}_\mu\{\cdot\}$ the expectation and variance for μ , respectively. Then, $f(\cdot)$ admits the following Sobol'-Hoeffding decomposition of $f(\cdot)$ in 2^d terms, see [10, 33],

$$f(\mathbf{x}) = f_0 + \sum_{i=1}^d f_i(x_i) + \sum_{i \leq j \leq d} f_{i,j}(x_i, x_j) + \sum_{i \leq j \leq k \leq d} f_{i,j,k}(x_i, x_j, x_k) + \dots + f_{1,\dots,d}(x_1, \dots, x_d). \quad (2.1)$$

For \mathcal{U} an index set, $\mathcal{U} \subset \{1, \dots, d\}$, denote by $\mathbf{x}_{\mathcal{U}}$ the vector with components x_i for $i \in \mathcal{U}$ and by $f_{\mathcal{U}}(\mathbf{x}_{\mathcal{U}})$ the corresponding term in the decomposition above (without further indication, we shall only consider ordered index sets). For a fixed f_0 , when we impose that

$$\forall i \in \mathcal{U}, \quad \int_{\mathcal{X}} f_{\mathcal{U}}(\mathbf{x}_{\mathcal{U}}) d\mu_i(x_i) = 0, \quad (2.2)$$

then the decomposition (2.1) is unique. Moreover, we have the orthogonality property

$$\forall \mathcal{U} \neq \mathcal{V}, \quad \mathcal{U}, \mathcal{V} \subset \{1, \dots, d\}, \quad \mathbf{E}_\mu\{f_{\mathcal{U}}(\mathbf{X}_{\mathcal{U}})f_{\mathcal{V}}(\mathbf{X}_{\mathcal{V}})\} = 0,$$

together with $f_0 = \mathbb{E}_\mu\{f(\mathbf{X})\}$. This orthogonality property implies that we can decompose the variance of $f(\mathbf{X})$ as

$$\begin{aligned} V = \text{var}_\mu\{f(\mathbf{X})\} &= \sum_{i=1}^d \text{var}_\mu\{f_i(X_i)\} + \sum_{i \leq j \leq d} \text{var}_\mu\{f_{i,j}(X_i, X_j)\} + \cdots + \text{var}_\mu\{f_{1,\dots,d}(X_1, \dots, X_d)\} \\ &= \sum_{\mathcal{U} \subset \{1, \dots, d\}} V_{\mathcal{U}}, \end{aligned}$$

where we have denoted $V_{\mathcal{U}} = \text{var}_\mu\{f_{\mathcal{U}}(\mathbf{X}_{\mathcal{U}})\}$. For any $\mathcal{U} \subset \{1, \dots, d\}$, (2.2) implies that

$$\mathbb{E}_\mu\{f(\mathbf{X})|\mathbf{X}_{\mathcal{U}}\} = f_0 + \sum_{\mathcal{V} \subseteq \mathcal{U}} f_{\mathcal{V}}(\mathbf{X}_{\mathcal{V}}),$$

so that $V_{\mathcal{U}} = \text{var}_\mu\{\mathbb{E}_\mu\{f(\mathbf{X})|\mathbf{X}_{\mathcal{U}}\}\} - \sum_{\mathcal{V} \subset \mathcal{U}} V_{\mathcal{V}}$, where the inclusion is strict on the right-hand side. The Sobol' sensitivity index associated with the index set \mathcal{U} is defined by

$$S_{\mathcal{U}} = \frac{V_{\mathcal{U}}}{V}.$$

Notice that $\sum_{\mathcal{U} \subset \{1, \dots, d\}} S_{\mathcal{U}} = 1$. The d first-order indices S_i (the $d(d-1)/2$ second-order indices $S_{i,j}$, respectively) correspond to $\mathcal{U} = \{i\}$, $i = 1, \dots, d$ ($\mathcal{U} = \{i, j\}$, $(i, j) \in \{1, \dots, d\}^2$, $i < j$, respectively). The closed index associated with \mathcal{U} is defined by

$$\underline{S}_{\mathcal{U}} = \frac{\text{var}_\mu\{\mathbb{E}_\mu\{f(\mathbf{X})|\mathbf{X}_{\mathcal{U}}\}\}}{V} = \sum_{\mathcal{V} \subseteq \mathcal{U}} S_{\mathcal{V}}. \quad (2.3)$$

Also of interest are the so-called total-effect indices,

$$\bar{S}_{\mathcal{U}} = \sum_{\mathcal{V} \cap \mathcal{U} \neq \emptyset} S_{\mathcal{V}} = 1 - \sum_{\mathcal{V} \cap \mathcal{U} = \emptyset} S_{\mathcal{V}} = 1 - \frac{\text{var}_\mu\{\mathbb{E}_\mu\{f(\mathbf{X})|\mathbf{X}_{\{1, \dots, d\} \setminus \mathcal{U}}\}\}}{V} = \frac{\mathbb{E}_\mu\{\text{var}_\mu\{f(\mathbf{X})|\mathbf{X}_{\{1, \dots, d\} \setminus \mathcal{U}}\}\}}{V},$$

among which in particular the d first-order total-effect indices $\bar{S}_i = \bar{S}_{\{i\}}$, $i = 1, \dots, d$. A group of variables $x_{\mathcal{U}}$ such that $\bar{S}_{\mathcal{U}} \approx 0$ can be considered as having negligible effect on the global behaviour of $f(\cdot)$, which thus allows dimension reduction.

2.2 Sobol' indices for tensor products of linear combinations of μ_i -orthonormal functions

For all $i = 1, \dots, d$, let $\{\phi_{i,\ell}(\cdot), \ell = 0, \dots, p_i\}$ denote a collection of $p_i + 1$ orthonormal functions for μ_i ; that is, such that

$$\int_{\mathcal{X}_i} \phi_{i,\ell}^2(x) d\mu_i(x) = 1 \text{ for all } \ell \text{ and } \int_{\mathcal{X}_i} \phi_{i,\ell}(x) \phi_{i,\ell'}(x) d\mu_i(x) = 0 \text{ for all } \ell' \neq \ell. \quad (2.4)$$

We suppose moreover that $\phi_{i,0}(x) \equiv 1$ for all i . Consider the tensor-product function defined by

$$f(\mathbf{x}) = \prod_{i=1}^d \left[\sum_{\ell=0}^{p_i} \alpha_{i,\ell} \phi_{i,\ell}(x) \right]. \quad (2.5)$$

It can be rewritten in the form of a linear regression model having $\prod_{i=1}^d (p_i + 1)$ parameters $\beta_{\underline{\ell}}$,

$$f(\mathbf{x}) = \sum_{\underline{\ell}} \beta_{\underline{\ell}} \psi_{\underline{\ell}}(\mathbf{x}),$$

where $\underline{\ell} = \{\ell_1, \dots, \ell_d\}$ denotes a multi index, with $\ell_i \in \{0, \dots, p_i\}$ for all $i = 1, \dots, d$, and where $\beta_{\underline{\ell}} = \prod_{i=1}^d \alpha_{i, \ell_i}$ and $\psi_{\underline{\ell}}(\mathbf{x}) = \prod_{i=1}^d \phi_{i, \ell_i}(x_i)$.

For any index set $\mathcal{U} \subset \{1, \dots, d\}$, since $\mathbb{E}_{\mu_i}\{\phi_{i, \ell}(X_i)\} = 0$ for all i and all $\ell \neq 0$, we have

$$\mathbb{E}_{\mu}\{f(\mathbf{X})|\mathbf{X}_{\mathcal{U}}\} = \beta_{\underline{0}} + \sum_{\underline{\ell} \in \mathbb{L}(\mathcal{U})} \beta_{\underline{\ell}} \psi_{\underline{\ell}}(\mathbf{X}),$$

where $\underline{0} = \{0, \dots, 0\}$ and $\mathbb{L}(\mathcal{U}) = \{\underline{\ell} \neq \underline{0} : \ell_i = 0 \text{ for all } i \notin \mathcal{U}\}$. Next, the orthonormality property (2.4) gives $\text{var}_{\mu}\{\psi_{\underline{\ell}}(\mathbf{X})\} = 1$ for $\underline{\ell} \neq \underline{0}$ and

$$\underline{S}_{\mathcal{U}} = \frac{\sum_{\underline{\ell} \in \mathbb{L}(\mathcal{U})} \beta_{\underline{\ell}}^2}{\sum_{\underline{\ell} \neq \underline{0}} \beta_{\underline{\ell}}^2},$$

from which we can easily compute $S_{\mathcal{V}}$ and $\bar{S}_{\mathcal{V}}$ for any index set \mathcal{V} , see Section 2.1. In particular,

$$S_i = \underline{S}_{\{i\}} \text{ and } \bar{S}_i = \frac{\sum_{\underline{\ell}: \ell_i \neq 0} \beta_{\underline{\ell}}^2}{\sum_{\underline{\ell} \neq \underline{0}} \beta_{\underline{\ell}}^2} \text{ for all } i = 1, \dots, d, \quad S_{i,j} = \underline{S}_{\{i,j\}} - S_i - S_j \text{ for all } i, j = 1, \dots, d.$$

When the $\phi_{i, \ell}(\cdot)$ in (2.5) are univariate polynomials $P_{i, \ell}(\cdot)$ of degree ℓ in a family of orthonormal polynomials for μ_i , the construction of Section 2.2 corresponds to the PCE approach in [35, 3, 1, 5].

3 A tensorised Bayesian linear model: theoretical construction

We shall construct a linear approximation model for $\mathbf{f}(\cdot)$, with orthonormal regression functions that satisfy the properties of Section 2.2, together with a prior on the parameters that will allow estimation from less observations than parameters. The construction relies on Gaussian RF models with a parametric trend given by orthonormal polynomials.

3.1 Construction of univariate models

We use the univariate orthonormal polynomials of the PCE model as trend functions for a univariate RF model; that is, for each $i = 1, \dots, d$ we consider

$$Y_{i,x} = \sum_{\ell=0}^{p_i} \alpha_{i, \ell} P_{i, \ell}(x) + Z_{i,x}, \quad (3.1)$$

where $(Z_{i,x})_{x \in \mathcal{X}_i}$ denotes a Gaussian RF indexed by \mathcal{X}_i , with zero mean ($\mathbb{E}\{Z_{i,x}\} = 0$ for all x) and covariance $\mathbb{E}\{Z_{i,x} Z_{i,x'}\} = K_i(x, x')$ for $x, x' \in \mathcal{X}_i$. We suppose that $K_i(\cdot, \cdot)$ is $\mu_i \times \mu_i$ -measurable and that $\mathbb{E}_{\mu_i}\{K_i(X, X)\} < +\infty$ for all i , and denote by T_{i, μ_i} the following linear operator on $L^2(\mathcal{X}_i, \mu_i)$:

$$\forall f \in L^2(\mathcal{X}_i, \mu_i), \quad \forall t \in \mathcal{X}_i, \quad T_{i, \mu_i}[f](t) = \int_{\mathcal{X}_i} f(x) K_i(t, x) d\mu_i(x) = \mathbb{E}_{\mu_i}\{f(X) K_i(t, X)\}.$$

For \mathbf{f} a vector of functions f_j in $L^2(\mathcal{X}, \mu_i)$, $j = 1, \dots, p$, with $\mathbf{f}(x) = (f_1(x), \dots, f_p(x))^T$ for all $x \in \mathcal{X}_i$, $T_{i, \mu_i}[\mathbf{f}]$ will denote the vectorized function with components $T_{i, \mu_i}[f_j]$.

Lemma 3.1. *The model (3.1) can be rewritten in the form of a linear regression model, as*

$$Y_{i,x} = \sum_{\ell=0}^{p_i} \tilde{\alpha}_{i,\ell} P_{i,\ell}(x) + \sum_{k \geq 1} \alpha'_{i,k} \varphi'_{i,k}(x) + \varepsilon_{i,0,x}, \quad (3.2)$$

where the $\tilde{\alpha}_{i,\ell}$, $\ell = 0, \dots, p_i$, form a set of $p_i + 1$ trend parameters, the $\alpha'_{i,k}$, $k \geq 1$, are independent centred normal random variables, and where $\varepsilon_{i,0,x}$ is a centred RF that satisfies $\mathbb{E}\{\alpha'_{i,k} \varepsilon_{i,0,x}\} = 0$ for all $x \in \mathcal{X}_i$. The regression functions $\varphi'_{i,k}(x)$ are orthonormal in $L^2(\mathcal{X}_i, \mu_i)$ and satisfy the orthogonality property $\mathbb{E}_{\mu_i}\{\varphi'_{i,k}(X) P_{i,\ell}(X)\} = 0$ for all $\ell = 1, \dots, p_i$ and all $k \geq 1$.

Proof. Following [14, Sect. 5.4], for each $i = 1, \dots, d$, we consider the orthogonal projection \mathbf{p}_i of $L^2(\mathcal{X}_i, \mu_i)$ onto the linear subspace \mathcal{T}_i spanned by the $P_{i,\ell}(\cdot)$, $\ell = 0, \dots, p_i$ and denote $\mathbf{q}_i = \text{id}_{L^2} - \mathbf{p}_i$. In matrix notation, we write $\mathbf{g}_i(x) = (P_{i,0}(x), \dots, P_{i,p_i}(x))^T$ and $\boldsymbol{\alpha}_i = (\alpha_{i,0}, \dots, \alpha_{i,p_i})^T$. From the orthonormality of the $P_{i,\ell}(\cdot)$, we can write, for $x \in \mathcal{X}_i$,

$$\mathbf{p}_i Z_{i,x} = \mathbf{g}_i^T(x) \mathbb{E}_{\mu_i}\{\mathbf{g}_i(X) Z_{i,X}\}, \quad (3.3)$$

with $\mathbb{E}\{\mathbf{p}_i Z_{i,x}\} = 0$ and, for $y \in \mathcal{X}_i$, $\mathbb{E}\{(\mathbf{p}_i Z_{i,x})(\mathbf{p}_i Z_{i,y})\} = \mathbf{g}_i^T(x) \mathbb{E}_{\mu_i}\{T_{i,\mu_i}[\mathbf{g}_i](X) \mathbf{g}_i^T(X)\} \mathbf{g}_i(y)$ and $\mathbb{E}\{(\mathbf{p}_i Z_{i,x}) Z_{i,y}\} = \mathbf{g}_i^T(x) T_{i,\mu_i}[\mathbf{g}_i](y)$. The model (3.1) can thus be written as

$$Y_{i,x} = \mathbf{g}_i^T(x) \boldsymbol{\alpha}_i + \mathbf{p}_i Z_{i,x} + \mathbf{q}_i Z_{i,x} = \mathbf{g}_i^T(x) \tilde{\boldsymbol{\alpha}}_i + \mathbf{q}_i Z_{i,x}, \quad (3.4)$$

with $\tilde{\boldsymbol{\alpha}}_i = \boldsymbol{\alpha}_i + \mathbb{E}_{\mu_i}\{\mathbf{g}_i(X) Z_{i,X}\}$. The covariance kernel of $(\mathbf{q}_i Z_{i,x})_{x \in \mathcal{X}_i}$ in (3.4) is equal to

$$\begin{aligned} \tilde{K}_i(x, y) = \mathbb{E}\{(\mathbf{q}_i Z_{i,x})(\mathbf{q}_i Z_{i,y})\} &= K_i(x, y) + \mathbf{g}_i^T(x) \mathbb{E}_{\mu_i}\{T_{i,\mu_i}[\mathbf{g}_i](X) \mathbf{g}_i^T(X)\} \mathbf{g}_i(y) \\ &\quad - T_{i,\mu_i}[\mathbf{g}_i^T](x) \mathbf{g}_i(y) - \mathbf{g}_i^T(x) T_{i,\mu_i}[\mathbf{g}_i](y). \end{aligned} \quad (3.5)$$

Note that in (3.4) we have orthogonality in $L^2(\mathcal{X}_i, \mu_i)$ between the realisations of $(\mathbf{q}_i Z_{i,x})_{x \in \mathcal{X}_i}$ and the trend subspace \mathcal{T}_i , with $\mathbf{p}_i Z_{i,x} \in \mathcal{T}_i$.

Consider now the integral operator associated with $\tilde{K}_i(\cdot, \cdot)$:

$$\forall f \in L^2(\mathcal{X}_i, \mu_i), \quad \forall t \in \mathcal{X}_i, \quad \tilde{T}_{i,\mu_i}[f](t) = \mathbb{E}_{\mu_i}\{f(X) \tilde{K}_i(t, X)\}.$$

By construction, \tilde{T}_{i,μ_i} satisfies $\tilde{T}_{i,\mu_i}[P_{i,\ell}] = 0$ for all $\ell \in \{0, \dots, p_i\}$. It can be diagonalised, and we denote by $\{\gamma_{i,1}, \gamma_{i,2}, \dots\}$ the set (at most countable) of its strictly positive eigenvalues, assumed to be ordered by decreasing values, and by $\varphi_{i,k} \in L^2(\mathcal{X}_i, \mu_i)$ the associated eigenfunctions. They satisfy $\tilde{T}_{i,\mu_i}[\varphi_{i,k}] = \gamma_{i,k} \varphi_{i,k}$ for all $k > 0$ and can be chosen orthonormal in $L^2(\mathcal{X}_i, \mu_i)$. Denote by $\varphi'_{i,k}$ their canonical extensions,

$$\forall x \in \mathcal{X}_i, \quad \varphi'_{i,k}(x) = \frac{1}{\gamma_{i,k}} \tilde{T}_{i,\mu_i}[\varphi_{i,k}](x), \quad k \geq 1. \quad (3.6)$$

The $\varphi'_{i,k}(\cdot)$ are defined over the whole \mathcal{X}_i , with $\varphi'_{i,k} = \varphi_{i,k}$ μ_i -almost everywhere, and satisfy the orthogonality property $\mathbb{E}_{\mu_i}\{\varphi'_{i,k}(X) P_{i,\ell}(X)\} = 0$ for all $\ell = 1, \dots, p_i$ and all $k \geq 1$.

The Karhunen-Loève expansion of $\mathbf{q}_i Z_{i,x}$ in (3.4) gives $\forall x \in \mathcal{X}_i$, $\mathbf{q}_i Z_{i,x} = \sum_{k \geq 1} \alpha'_{i,k} \varphi'_{i,k}(x) + \varepsilon_{i,0,x}$, where the $\alpha'_{i,k}$, $k \geq 1$, are mutually orthogonal normal random variables $\mathcal{N}(0, \gamma_{i,k})$ and where $\varepsilon_{i,0,x}$ is a centred RF satisfying $\mathbb{E}\{\alpha'_{i,k} \varepsilon_{i,0,x}\} = 0$ for all $x \in \mathcal{X}_i$. This concludes the proof of the lemma. (Note that $\varepsilon_{i,0,x}$ has covariance $\tilde{K}_i(x, x') - \sum_{k \geq 1} \gamma_{i,k} \varphi'_{i,k}(x) \varphi'_{i,k}(x')$, and cannot be ignored when μ_i is replaced by a finitely supported measure $\hat{\mu}_i$ and $Y_{i,x}$ is used out of the support of $\hat{\mu}_i$, see Section 4.) ■

3.2 Construction of a tensorised BLM

We set a prior on the $\tilde{\alpha}_{i,\ell}$ in (3.2), and suppose that $\tilde{\boldsymbol{\alpha}}_i = (\tilde{\alpha}_{i,0}, \dots, \tilde{\alpha}_{i,p_i})^T$ is normally distributed $\mathcal{N}(\mathbf{0}, \mathbf{D}_i)$, with $\mathbf{D}_i = \text{diag}\{\vartheta_{i,\ell}, \ell = 0, \dots, p_i\}$, for all $i = 1, \dots, d$. The choice of the $\vartheta_{i,\ell}$ is discussed in Section 4.3. Consider the separable kernel defined by $K'(\mathbf{x}, \mathbf{y}) = \prod_{i=1}^d K'_i(x_i, y_i)$, where

$$K'_i(x, y) = \tilde{K}_i(x, y) + \sum_{\ell=0}^{p_i} \vartheta_{i,\ell} P_{i,\ell}(x) P_{i,\ell}(y), \quad (3.7)$$

with $\tilde{K}_i(x, y)$ given by (3.5). The eigenvalues and eigenfunctions of the operator $T_\mu[f]$, defined by $T_\mu[f](\mathbf{t}) = \mathbb{E}_\mu\{f(\mathbf{X})K'(\mathbf{t}, \mathbf{X})\}$, $f \in L^2(\mathcal{X}, \mu)$, $\mathbf{t} \in \mathcal{X}$, are products of eigenvalues and eigenfunctions of the operators associated with the $K'_i(\cdot, \cdot)$. The Karhunen-Loève expansion of the centred Gaussian RF with covariance $K'(\cdot, \cdot)$ yields the following tensorised version of model (3.2):

$$Y_{\mathbf{x}} = \sum_{\underline{\ell} \in \mathbb{N}^d} \beta_{\underline{\ell}} \psi_{\underline{\ell}}(\mathbf{x}) + \varepsilon_{0,\mathbf{x}}, \quad (3.8)$$

where $\underline{\ell} = \{\ell_1, \dots, \ell_d\}$ with $\ell_i \in \mathbb{N}$ for all i , the $\beta_{\underline{\ell}}$ are independent random variables $\mathcal{N}(0, \Lambda_{\underline{\ell}})$, and where $\varepsilon_{0,\mathbf{x}}$ is a centred RF with covariance $\mathbb{E}\{\varepsilon_{0,\mathbf{x}}\varepsilon_{0,\mathbf{y}}\} = \prod_{i=1}^d K'_i(x_i, y_i) - \sum_{\underline{\ell} \in \mathbb{N}^d} \Lambda_{\underline{\ell}} \psi_{\underline{\ell}}(\mathbf{x}) \psi_{\underline{\ell}}(\mathbf{y})$, with

$$\begin{aligned} \Lambda_{\underline{\ell}} &= \prod_{i=1}^d \lambda_{i,\ell_i}, \quad \psi_{\underline{\ell}}(\mathbf{x}) = \prod_{i=1}^d \phi_{i,\ell_i}(x_i) \text{ for any } \mathbf{x} \in \mathcal{X}, \\ \phi_{i,\ell}(\cdot) &= \begin{cases} P_{i,\ell}(\cdot) & \text{for } \ell = 0, \dots, p_i, \\ \varphi'_{i,\ell-p_i}(\cdot) & \text{for } \ell \geq p_i + 1, \end{cases} \quad \lambda_{i,\ell}(\cdot) = \begin{cases} \vartheta_{i,\ell} & \text{for } \ell = 0, \dots, p_i, \\ \gamma_{i,\ell-p_i} & \text{for } \ell \geq p_i + 1, \end{cases} \end{aligned} \quad (3.9)$$

and $\gamma_{i,1} \geq \gamma_{i,2} \geq \dots$ the eigenvalues defined in the proof of Lemma 3.1. When truncating the sum in (3.8) to $\underline{\ell}$ in a given finite subset \mathbb{L} of \mathbb{N}^d , we obtain the model $Y_{\mathbf{x}} = \sum_{\underline{\ell} \in \mathbb{L}} \beta_{\underline{\ell}} \psi_{\underline{\ell}}(\mathbf{x}) + \varepsilon_{\mathbf{x}}$, where now $\mathbb{E}\{\varepsilon_{\mathbf{x}}\varepsilon_{\mathbf{y}}\} = \prod_{i=1}^d K'_i(x_i, y_i) - \sum_{\underline{\ell} \in \mathbb{L}} \Lambda_{\underline{\ell}} \psi_{\underline{\ell}}(\mathbf{x}) \psi_{\underline{\ell}}(\mathbf{y})$. The choice of \mathbb{L} will be discussed in Section 4.4.

Finally, the BLM we shall use for sensitivity analysis is given by

$$Y_{\mathbf{x}} = \sum_{\underline{\ell} \in \mathbb{L}} \beta_{\underline{\ell}} \psi_{\underline{\ell}}(\mathbf{x}) + \varepsilon'_{\mathbf{x}}, \quad (3.10)$$

where we have replaced the errors $\varepsilon_{\mathbf{x}}$ by uncorrelated ones $\varepsilon'_{\mathbf{x}}$, such that $\mathbb{E}\{\varepsilon'_{\mathbf{x}}\varepsilon'_{\mathbf{y}}\} = 0$ for $\mathbf{x} \neq \mathbf{y}$ and

$$\forall \mathbf{x} \in \mathcal{X}, \quad s^2(\mathbf{x}) = \mathbb{E}\{(\varepsilon'_{\mathbf{x}})^2\} = \mathbb{E}\{(\varepsilon_{\mathbf{x}})^2\} = \prod_{i=1}^d K'_i(x_i, x_i) - \sum_{\underline{\ell} \in \mathbb{L}} \Lambda_{\underline{\ell}} \psi_{\underline{\ell}}^2(\mathbf{x}). \quad (3.11)$$

Following the results in Section 2.1, the estimation of the parameters $\beta_{\underline{\ell}}$ in (3.10) from evaluations of $f(\cdot)$ at a given set of design points will provide estimates of Sobol' indices; see Section 5.

Remark 3.1. We may also consider the estimation of $\beta_{\underline{\ell}}$ in the model with correlated errors $\varepsilon_{\mathbf{x}}$. Estimation from a n -point design then requires the calculation and manipulation of a $n \times n$ correlation matrix, whereas only its n diagonal terms need to be used for the model (3.10). Numerical experiments indicate that the gain in precision is negligible when considering correlations. Moreover, the approximate model with uncorrelated errors allows the selection of observation points adapted to the estimation of Sobol' indices by classical approaches for optimal design, see Section 6. \triangleleft

4 Practical implementation via quadrature approximation

The $\varphi'_{i,k}(\cdot)$ and associated eigenvalues $\gamma_{i,k}$ in (3.2) are usually unknown, and we need to resort to numerical approximations. A convenient practical implementation consists in replacing the measures μ_i by quadrature approximations

$$\hat{\mu}_i = \sum_{j=1}^{q_i} w_{i,j} \delta_{x_{i,j}}.$$

For all $i = 1, \dots, d$, denote $\mathbf{W}_i = \text{diag}\{w_{i,j}, j = 1, \dots, q_i\}$ and \mathbf{Q}_i (respectively, $\tilde{\mathbf{Q}}_i$) the matrix with j, k term $\{\mathbf{Q}_i\}_{j,k} = K_i(x_{i,j}, x_{i,k})$ (respectively, $\{\tilde{\mathbf{Q}}_i\}_{j,k} = \tilde{K}_i(x_{i,j}, x_{i,k})$) for $j, k = 1, \dots, q_i$. We assume that $\prod_{i=1}^d q_i \gg n$, the projected number of evaluations of $\mathbf{f}(\cdot)$.

Remark 4.1. The substitution of $\hat{\mu}_i$ for μ_i has the consequence that the basis functions $\phi_{i,\ell}$ used in (3.9) are orthonormal for $\hat{\mu}_i$; Sobol' indices will therefore be estimated for the measure $\hat{\mu} = \bigotimes_{i=1}^d \hat{\mu}_i$. However, since $\hat{\mu}$ has $\prod_{i=1}^d q_i$ support points, the q_i do not need to be very large to be able to neglect this quadrature effect, and $q_i \approx 100$ seems to be enough in most cases, see Sections 4.6 and 7. On the other hand, the $\hat{\mu}_i$ may also correspond to empirical measures obtained from historical data, a situation where q_i may naturally take large values. \triangleleft

4.1 Construction of $\tilde{\mathbf{Q}}_i$

For each $i = 1, \dots, d$ we must construct polynomials $P_{i,\ell}(\cdot)$, of degrees $\ell = 0, \dots, p_i \leq q_i - 1$, orthonormal for the measure $\hat{\mu}_i$. Direct calculation shows that orthonormality implies (up to an arbitrary sign change)

$$P_{i,0}(x) = 1 \quad \text{and} \quad P_{i,\ell}(x) = \frac{\det \begin{pmatrix} 1 & m_{i,1} & \cdots & m_{i,\ell} \\ m_{i,1} & m_{i,2} & \cdots & m_{i,\ell+1} \\ \vdots & \vdots & \ddots & \vdots \\ m_{i,\ell-1} & m_{i,\ell} & \cdots & m_{i,2\ell-1} \\ 1 & x & \cdots & x^\ell \end{pmatrix}}{\det^{1/2}(\mathbf{M}_{i,\ell}) \det^{1/2}(\mathbf{M}_{i,\ell-1})} \quad \text{for } \ell \geq 1,$$

where, for any $\ell \in \mathbb{N}$, $\mathbf{M}_{i,\ell}$ is the $(\ell+1) \times (\ell+1)$ moment matrix with j, k term $\{\mathbf{M}_{i,\ell}\}_{j,k} = m_{i,j+k-2}$ and $m_{i,k} = \mathbb{E}_{\hat{\mu}_i}\{X^k\}$ for all k . Denote by \mathbf{G}_i the $q_i \times (p_i + 1)$ matrix with j, ℓ term $P_{i,\ell}(x_{i,j})$. It satisfies $\mathbf{G}_i^T \mathbf{W}_i \mathbf{G}_i = \mathbf{I}_{p_i+1}$ and we have, from the definition (3.5) of $\tilde{K}_i(\cdot, \cdot)$,

$$\tilde{\mathbf{Q}}_i = \mathbf{Q}_i + \mathbf{G}_i \mathbf{G}_i^T \mathbf{W}_i \mathbf{Q}_i \mathbf{W}_i \mathbf{G}_i \mathbf{G}_i^T - \mathbf{G}_i \mathbf{G}_i^T \mathbf{W}_i \mathbf{Q}_i - \mathbf{Q}_i \mathbf{W}_i \mathbf{G}_i \mathbf{G}_i^T, \quad (4.1)$$

from which we can readily check that $\tilde{\mathbf{Q}}_i \mathbf{W}_i \mathbf{G}_i = \mathbf{O}_{q_i, (p_i+1)}$, the $q_i \times (p_i + 1)$ null matrix.

4.2 Calculation of $\psi_\ell(\mathbf{x})$ and $s^2(\mathbf{x})$

To calculate $\psi_\ell(\mathbf{x})$ in (3.10) we need to compute the $\varphi'_{i,k}(x_i)$ and the $\gamma_{i,k}$ in (3.9). Also, the calculation of the variance $s^2(\mathbf{x})$ of $\varepsilon'_\mathbf{x}$ requires the computation of the $K'_i(x_i, x_i)$, see (3.11). As shown below, the use of quadrature approximations $\hat{\mu}_i$ reduces these computations to a few matrices and vectors manipulations.

Diagonalisation of $q_i \times q_i$ matrices The diagonalisation of $\mathbf{W}_i^{1/2} \tilde{\mathbf{Q}}_i \mathbf{W}_i^{1/2}$ yields a matrix $\tilde{\mathbf{\Phi}}_i$ of eigenvectors and a diagonal matrix $\mathbf{\Gamma}_i$ of associated eigenvalues (sorted by decreasing values) that satisfy $\mathbf{W}_i^{1/2} \tilde{\mathbf{Q}}_i \mathbf{W}_i^{1/2} = \tilde{\mathbf{\Phi}}_i \mathbf{\Gamma}_i \tilde{\mathbf{\Phi}}_i^T$, with $\tilde{\mathbf{\Phi}}_i^T \tilde{\mathbf{\Phi}}_i = \mathbf{I}_{q_i}$, the $q_i \times q_i$ identity matrix. Denote $\mathbf{\Phi}_i = \mathbf{W}_i^{-1/2} \tilde{\mathbf{\Phi}}_i$; it satisfies $\mathbf{\Phi}_i^T \mathbf{W}_i \mathbf{\Phi}_i = \mathbf{I}_{q_i}$, $\tilde{\mathbf{Q}}_i = \mathbf{\Phi}_i \mathbf{\Gamma}_i \mathbf{\Phi}_i^T$ and $\tilde{\mathbf{Q}}_i \mathbf{W}_i \mathbf{\Phi}_i = \mathbf{\Phi}_i \mathbf{\Gamma}_i$, so that $\mathbf{G}_i^T \mathbf{W}_i \mathbf{\Phi}_i = \mathbf{O}_{(p_i+1), q_i}$. The columns of $\mathbf{\Phi}_i$ correspond to the eigenfunctions $\varphi_{i,k}$ in the proof of Lemma 3.1.

Quadrature designs Following [14], we call *quadrature design* of size n a collection $\mathcal{D}_n = \{\mathbf{x}_1, \dots, \mathbf{x}_n\}$ of n points of \mathcal{X} such that $\{\mathbf{x}_\ell\}_i$ is included in the support of $\hat{\mu}_i$ for all $\ell = 1, \dots, n$ and $i = 1, \dots, d$. When \mathbf{x} belongs to a quadrature design, its i th component x_i is therefore the j th support point of μ_i , for some $j \in \{1, \dots, q_i\}$; $\varphi'_{i,k}(x_i)$ and $\gamma_{i,k}$ in (3.9) are then respectively given by $\{\mathbf{\Phi}_i\}_{j,k}$ and by the k th diagonal element of $\mathbf{\Gamma}_i$. Also, from (3.7), $K'_i(x_i, x_i)$ in (3.11) is given by

$$K'_i(x_i, x_i) = \{\tilde{\mathbf{Q}}_i\}_{j,j} + \sum_{\ell=0}^{p_i} \vartheta_{i,\ell} P_{i,\ell}^2(x_i) = \sum_{\ell=1}^{q_i} \gamma_{i,\ell} \{\mathbf{\Phi}_i\}_{j,\ell}^2 + \sum_{\ell=0}^{p_i} \vartheta_{i,\ell} P_{i,\ell}^2(x_i).$$

General designs When \mathbf{x} is an arbitrary point in \mathcal{X} , x_i is generally not in the support of $\hat{\mu}_i$. To calculate $\psi_\ell(\mathbf{x})$, see (3.9), we therefore need to compute the canonical extensions $\varphi'_{i,\ell}(x_i)$ defined by (3.6). Denote

$$\mathbf{k}_i(x) = [K_i(x, x_{i,1}), \dots, K_i(x, x_{i,q_i})]^T \text{ and } \tilde{\mathbf{k}}_i(x) = [\tilde{K}_i(x, x_{i,1}), \dots, \tilde{K}_i(x, x_{i,q_i})]^T.$$

From (3.6), $\varphi'_{i,\ell}(x_i)$ corresponds to the ℓ th component of $\phi'_i(x_i) = \mathbf{\Gamma}_i^{-1} \mathbf{\Phi}_i^T \mathbf{W}_i \tilde{\mathbf{k}}_i(x_i)$, where

$$\tilde{\mathbf{k}}_i(x) = \mathbf{k}_i(x) + \mathbf{G}_i \mathbf{G}_i^T \mathbf{W}_i \mathbf{Q}_i \mathbf{W}_i \mathbf{G}_i \mathbf{g}_i(x) - \mathbf{Q}_i \mathbf{W}_i \mathbf{G}_i \mathbf{g}_i(x) - \mathbf{G}_i \mathbf{G}_i^T \mathbf{W}_i \mathbf{k}_i(x),$$

for all $i = 1, \dots, d$ and all $x \in \mathcal{X}_i$; see (3.5). Since $\mathbf{\Phi}_i^T \mathbf{W}_i \mathbf{G}_i = \mathbf{O}_{q_i, (p_i+1)}$, the expression of $\phi'_i(x_i)$ simplifies into

$$\phi'_i(x_i) = \mathbf{\Gamma}_i^{-1} \mathbf{\Phi}_i^T \mathbf{W}_i \mathbf{k}_i(x_i) - \mathbf{\Gamma}_i^{-1} \mathbf{\Phi}_i^T \mathbf{W}_i \mathbf{Q}_i \mathbf{W}_i \mathbf{G}_i \mathbf{g}_i(x_i). \quad (4.2)$$

From (3.7), we also get

$$K'_i(x_i, x_i) = K_i(x_i, x_i) + \mathbf{g}_i^T(x_i) \mathbf{G}_i^T \mathbf{W}_i \mathbf{Q}_i \mathbf{W}_i \mathbf{G}_i \mathbf{g}_i(x_i) - 2 \mathbf{g}_i^T(x_i) \mathbf{G}_i^T \mathbf{W}_i \mathbf{k}_i(x_i) + \sum_{\ell=0}^{p_i} \vartheta_{i,\ell} P_{i,\ell}^2(x_i). \quad (4.3)$$

Remark 4.2. When $p_i \geq 1$, if orthogonal polynomials $P'_{i,\ell}(\cdot)$ for μ_i are known, it is tempting to directly use $\{\mathbf{G}_i\}_{j,\ell} = P'_{i,\ell}(x_{i,j})$ to avoid the construction in Section 4.1. The orthogonal projection (3.3) must then be modified into $\mathbf{p}_i Z_{i,x} = \mathbf{g}_i^T(x) \mathbf{M}_{\mathbf{g}_i}^{-1} \mathbf{E}_{\mu_i} \{\mathbf{g}_i(X) Z_{i,X}\}$, with $\mathbf{M}_{\mathbf{g}_i}$ the $p_i \times p_i$ Gram matrix $\mathbf{E}_{\mu_i} \{\mathbf{g}_i(X) \mathbf{g}_i^T(X)\}$. (We suppose that μ_i is such that $\mathbf{M}_{\mathbf{g}_i}$ is invertible.) The expression of $\tilde{K}_i(x, y)$ must be modified accordingly, into

$$\begin{aligned} \tilde{K}_i(x, y) &= K_i(x, y) + \mathbf{g}_i^T(x) \mathbf{M}_{\mathbf{g}_i}^{-1} \mathbf{E}_{\mu_i} \{T_{i,\mu_i}[\mathbf{g}_i](X) \mathbf{g}_i^T(X)\} \mathbf{M}_{\mathbf{g}_i}^{-1} \mathbf{g}_i(y) \\ &\quad - T_{i,\mu_i}[\mathbf{g}_i^T](x) \mathbf{M}_{\mathbf{g}_i}^{-1} \mathbf{g}_i(y) - \mathbf{g}_i^T(x) \mathbf{M}_{\mathbf{g}_i}^{-1} T_{i,\mu_i}[\mathbf{g}_i](y), \end{aligned}$$

and (4.1) becomes

$$\tilde{\mathbf{Q}}_i = \mathbf{Q}_i + \mathbf{G}_i \mathbf{M}_{\mathbf{g}_i}^{-1} \mathbf{G}_i^T \mathbf{W}_i \mathbf{Q}_i \mathbf{W}_i \mathbf{G}_i \mathbf{M}_{\mathbf{g}_i}^{-1} \mathbf{G}_i^T - \mathbf{G}_i \mathbf{M}_{\mathbf{g}_i}^{-1} \mathbf{G}_i^T \mathbf{W}_i \mathbf{Q}_i - \mathbf{Q}_i \mathbf{W}_i \mathbf{G}_i \mathbf{M}_{\mathbf{g}_i}^{-1} \mathbf{G}_i^T.$$

Also, when \mathbf{x} is not a quadrature point, (4.2) and (4.3) must be respectively modified into

$$\phi'_i(x_i) = \mathbf{\Gamma}_i^{-1} \mathbf{\Phi}_i^T \mathbf{W}_i \mathbf{k}_i(x_i) - \mathbf{\Gamma}_i^{-1} \mathbf{\Phi}_i^T \mathbf{W}_i \mathbf{Q}_i \mathbf{W}_i \mathbf{G}_i \mathbf{M}_{\mathbf{g}_i}^{-1} \mathbf{g}_i(x_i) \quad (4.4)$$

and $K'_i(x_i, x_i) = K_i(x_i, x_i) + \mathbf{g}_i^T(x_i) \mathbf{M}_{\mathbf{g}_i}^{-1} \mathbf{G}_i^T \mathbf{W}_i \mathbf{Q}_i \mathbf{W}_i \mathbf{G}_i \mathbf{M}_{\mathbf{g}_i}^{-1} \mathbf{g}_i(x_i) - 2 \mathbf{g}_i^T(x_i) \mathbf{M}_{\mathbf{g}_i}^{-1} \mathbf{G}_i^T \mathbf{W}_i \mathbf{k}_i(x_i) + \sum_{\ell=0}^{p_i} \vartheta_{i,\ell} [P'_{i,\ell}(x_i)]^2$. Note, however, that the $P'_{i,\ell}(\cdot)$ being not orthonormal for $\hat{\mu}_i$, contrarily to the eigenfunctions $\varphi'_{i,\ell}(x_i)$, this may perturb the estimation of Sobol' indices and this approach is not recommended. \triangleleft

4.3 Choice of $\vartheta_{i,\ell}$, $\ell = 0, \dots, p_i$

The selection of eigenfunctions $\psi_\ell(\cdot)$ in (3.10) will rely on the energy of each component, measured by the associated eigenvalues, see Section 4.4. It is therefore important to choose values of $\vartheta_{i,\ell}$ in (3.9) large enough to ensure that important polynomial trend functions will be kept in the model, but not too large to allow the preference of other eigenfunctions if necessary. There is some arbitrariness in this construction, but we think the suggestion below is suitable in most situations.

Using stationary kernels $K_i(\cdot, \cdot)$, we can assume (without any loss of generality) that $K_i(x, x) = 1$ for all $x \in \mathcal{X}_i$ and each $i = 1, \dots, d$. Indeed, in (3.10), we can write the variance of β_ℓ as $\sigma^2 \Lambda_\ell$ and the variance of $\varepsilon'_\mathbf{x}$ as $s^2(\mathbf{x}) = \sigma^2 \left[\prod_{i=1}^d K'_i(x_i, x_i) - \sum_{\ell \in \mathbb{L}} \Lambda_\ell \psi_\ell^2(\mathbf{x}) \right]$ for some positive scalar σ^2 , and then estimate σ^2 from the data; see Section 5.2. Since $\sum_{k \geq 1} \gamma_{i,k} = \mathbf{E}_{\mu_i} \{ \tilde{K}_i(X, X) \} \leq \mathbf{E}_{\mu_i} \{ K_i(X, X) \}$, see [14], we have $\sum_{k \geq 1} \gamma_{i,k} \leq 1$, and we can take $\vartheta_{i,0} = 1$ for all i . When $p_i \geq 1$, in order to favour the selection of low degree polynomials, we suggest to take $\vartheta_{i,\ell} = \kappa_i^\ell$ with $\kappa_i = \gamma_{i,1}^{1/(1+p_i)}$, so that $\vartheta_{i,\ell} > \gamma_{i,k}$ for all $\ell = 0, \dots, p_i$ and all $k \geq 1$.

4.4 Choice of the truncation set \mathbb{L}

In PCE, when considering the tensor product of polynomials up to degree p_i in variable x_i , the model can have up to $\prod_{i=1}^d (1 + p_i)$ terms. A rather usual approach consists in favouring simple models by setting a constraint on the total degree D of the polynomial in d variables; the resulting model has then $\binom{d+D}{d}$ parameters (the cardinality of the set $\{\underline{\ell} = \{\ell_1, \dots, \ell_d\} \in \mathbb{N}^d : \sum_{\ell=1}^d \ell_\ell \leq D\}$).

Here we suggest to base the selection of terms in (3.10) on the ranking of the eigenvalues Λ_ℓ . We first choose a number $N \leq \bar{N} = \prod_{i=1}^d (p_i + q_i + 1)$ that specifies the size of the model; that is, the number of functions we want to consider — a value of N of the same order of magnitude as the projected number of evaluations of $\mathbf{f}(\cdot)$ seems reasonable. Let $\Lambda_{\underline{\ell}_1} \geq \dots \geq \Lambda_{\underline{\ell}_k} \geq \Lambda_{\underline{\ell}_{k+1}} \geq \dots$ denote the ordered sequence of the $\Lambda_\ell = \prod_{i=1}^d \lambda_{i,\ell_i}$, with $\underline{\ell} = \{\ell_1, \dots, \ell_d\} \in \mathbb{N}^d$, where we set $\Lambda_{\{\ell_1, \dots, \ell_d\}} = 0$ when $\ell_i > p_i + q_i + 1$ for some i . Note that $\underline{\ell}_1 = \underline{0} = \{0, \dots, 0\}$ and $\Lambda_{\underline{\ell}_1} = 1$; see Section 4.3. The truncation set is then

$$\mathbb{L}_N = \{\underline{\ell}_1, \dots, \underline{\ell}_M \in \mathbb{N}^d, \text{ with } M \text{ the smaller integer } \geq N \text{ such that } \Lambda_{\underline{\ell}_M} < \Lambda_{\underline{\ell}_{M+1}}\}. \quad (4.5)$$

Remark 4.3. We do not need to compute all the \bar{N} values $\Lambda_{\underline{\ell}_k}$, and the construction of \mathbb{L}_N can be sequential since the $\lambda_{i,k}$ are ordered (by decreasing values) for each i . Also, due to the truncation operated in the construction of \mathbb{L}_N , in theory we do not need to compute all q_i eigenpairs in the spectral decomposition of Section 4.2. The resulting computational gain may be marginal when each approximation $\hat{\mu}_i$ has a small numbers q_i of components, but may be significant when the $\hat{\mu}_i$ correspond to empirical data; see Remark 4.1. \triangleleft

Remark 4.4. In the special case where all $\hat{\mu}_i$ are identical and are supported on q points, and $p_i = p$ for all i , all matrices \mathbf{Q}_i are identical, and the same is true for \mathbf{Q}_i , $\mathbf{\Phi}_i$, $\mathbf{\Gamma}_i$, etc. (a single

diagonalisation is thus required, see Section 4.2). The model (3.10) has m^d terms at most, with $m = p + q + 1$. Each $\Lambda_{\underline{\ell}}$ can be written as

$$\Lambda_{\underline{\ell}} = \lambda_0^{a_0} \times \cdots \times \lambda_{m-1}^{a_{m-1}}, \quad (4.6)$$

with $a_k = |\{i : \ell_i = k\}|$ and $\sum_{k=0}^{m-1} a_k = d$. The $\Lambda_{\underline{\ell}}$ can thus take $\binom{d+m-1}{m-1}$ different values at most; there are at least $d!/(a_0! \times \cdots \times a_{m-1}!)$ different $\psi_{\underline{\ell}}(\cdot)$ associated with the same $\Lambda_{\underline{\ell}}$ given by (4.6). \triangleleft

4.5 The special case $p_i = 0$

In absence of reliable prior information on the behaviour of $f(\cdot)$, we recommend to only use a constant term for the trend; that is, to take $p_i = 0$ for all i . Then, $\mathbf{g}_i(x) = 1$ for all i and x , and the reduced kernel $\tilde{K}_i(x, y)$ is given by $\tilde{K}_i(x, y) = K_i(x, y) + \mathbf{E}_{\mu_i}\{K_i(X, Y)\} - \mathbf{E}_{\mu_i}\{K_i(x, X)\} - \mathbf{E}_{\mu_i}\{K_i(y, X)\}$; (4.1) becomes $\tilde{\mathbf{Q}}_i = \mathbf{Q}_i + \mathbf{1}_{q_i}(\mathbf{1}_{q_i}^T \mathbf{W}_i \mathbf{Q}_i \mathbf{W}_i \mathbf{1}_{q_i}) \mathbf{1}_{q_i}^T - \mathbf{1}_{q_i} \mathbf{1}_{q_i}^T \mathbf{W}_i \mathbf{Q}_i - \mathbf{Q}_i \mathbf{W}_i \mathbf{1}_{q_i} \mathbf{1}_{q_i}^T$, with $\mathbf{1}_{q_i}$ the q_i -dimensional vector of ones, and (4.2) and (4.3) respectively become $\phi'_i(x) = \mathbf{\Gamma}_i^{-1} \mathbf{\Phi}_i^T \mathbf{W}_i \mathbf{k}_i(x) - \mathbf{\Gamma}_i^{-1} \mathbf{\Phi}_i^T \mathbf{W}_i \mathbf{Q}_i \mathbf{W}_i \mathbf{1}_{q_i}$ and $K'_i(x, x) = K_i(x, x) + \mathbf{1}_{q_i}^T \mathbf{W}_i \mathbf{Q}_i \mathbf{W}_i \mathbf{1}_{q_i} - 2 \mathbf{k}_i(x)^T \mathbf{W}_i \mathbf{1}_{q_i} + \sum_{\ell=0}^{p_i} \vartheta_{i,\ell} P_{i,\ell}^2(x)$. We only need to choose $\vartheta_{i,0}$ in (3.9), and we can take $\vartheta_{i,0} = 1$ for all i ; see Section 4.3.

4.6 Numerical illustrations

Consider the Matérn 3/2 covariance function, given by $K_{3/2}(x, y; \theta) = (1 + \sqrt{3}\theta|x-y|) \exp(-\sqrt{3}\theta|x-y|)$; see [34, Chap. 2]. A zero-mean Gaussian process with this covariance is once mean-square differentiable and has differentiable sample paths almost surely. Suppose that μ_1 is the uniform measure on $[0, 1]$, and consider the discrete approximation $\hat{\mu}_1(q_1)$ that puts weight $1/q_1$ on each of the q_1 points $x_{1,j} = (j-1)/(q_1-1)$, $j = 1, \dots, q_1$. We take $p_1 = 2$, and the polynomials $P_{1,j}(\cdot)$, orthonormal for μ_1 , are $P_{1,0}(x) = 1$, $P_{1,1}(x) = \sqrt{3}(2x-1)$ and $P_{1,2}(x) = \sqrt{5}(6x^2-6x+1)$.

Figure 1-left shows the values of the components of the first three eigenvectors $\varphi_{1,\ell}(x_{1,j}) = \{\Phi_1\}_{j,\ell}$, $j = 1, \dots, q_1 = 20$, of the reduced kernel for $\ell = 1$ (triangles), $\ell = 2$ (circles) and $\ell = 3$ (crosses), when $\theta = 2$ (top) and $\theta = 20$ (bottom). Their canonical extensions $\varphi'_{1,\ell}(x)$, $x \in [0, 1]$, obtained from (4.4), are plotted in blue dashed line. They are orthonormal for $\hat{\mu}_1(20)$, and close to being orthonormal and orthogonal to the $P_{i,\ell}(x)$ (plotted in red solid line) for μ_1 ; see Table 1. The components of the first three eigenvectors obtained when $q_1 = 100$ are indicated by dots. One may notice the good agreement with the canonical extensions $\varphi'_{1,\ell}(x)$ based on 20 points only. We shall use $q_i = 100$ in the examples of Section 7 to ensure quasi-orthonormality of the $\psi_{\underline{\ell}}(\cdot)$ for μ_1 in (3.10), see Table 1.

Figure 1-right shows the values of the $\lambda_{1,\ell}$ in (3.9), $\ell = 0, \dots, 10$, for $q_1 = 20$. The eigenvalues $\gamma_{1,\ell}$ associated with the $\varphi'_{1,\ell}$ are indicated by stars; the values of $\vartheta_{1,\ell} = \gamma_{1,1}^{\ell/(1+p_1)} = \gamma_{1,1}^{\ell/3}$ in (3.9) (see Section 4.3) for $\ell = 0, 1, 2$ are indicated by triangles. We can see that θ (the inverse of the correlation length) has a moderate influence on the first eigenfunctions of the decomposition, but the decrease of eigenvalues is significantly slower for $\theta = 20$ (bottom) than for $\theta = 2$ (top), which has a noticeable impact on the prior distribution of Sobol' indices; see Section 7. The choice of θ should preferably agree with prior information on the fluctuations of $f(\cdot)$. In absence of such prior knowledge, a possible guideline is to select a value of θ compatible with the projected number n of function evaluations: a model with about n components should be able to capture the global behaviour of $f(\cdot)$ over \mathcal{X} . Suppose that a unique kernel is used for all dimensions, and define

$$\rho(\theta) = \frac{\sum_{k=1}^n \Lambda_{\ell_k}}{\sum_k \Lambda_{\ell_k}} = \frac{\sum_{k=1}^n \Lambda_{\ell_k}}{\prod_{i=1}^d \left(\sum_{\ell=1}^{p_i+q_i+1} \lambda_{i,\ell} \right)}, \quad (4.7)$$

	$q_i = 20$			$q_i = 100$		
	$\varphi'_{1,1}$	$\varphi'_{1,2}$	$\varphi'_{1,3}$	$\varphi'_{1,1}$	$\varphi'_{1,2}$	$\varphi'_{1,3}$
$P_{1,0}$	≈ 0	0.0803	≈ 0	≈ 0	-0.0180	≈ 0
$P_{1,1}$	-0.1468	≈ 0	0.1447	0.0304	≈ 0	0.0322
$P_{1,2}$	≈ 0	0.1879	≈ 0	≈ 0	-0.0408	≈ 0
$\varphi'_{1,1}$	0.9208	≈ 0	0.1295	0.9799	≈ 0	-0.0320
$\varphi'_{1,2}$.	0.9314	≈ 0	.	0.9779	≈ 0
$\varphi'_{1,3}$.	.	0.9247	.	.	0.9762

Table 1: Inner products $\langle \phi_{1,\ell}, \phi_{1,\ell'} \rangle_{L^2(\mathcal{X}, \mu)}$, computed by numerical integration, between regression functions used in (3.2). The canonical extensions $\varphi'_{1,j}(\cdot)$ are based on a q_i -point quadrature approximation of μ uniform on $[0, 1]$ and the covariance $K_{3/2}(x, y; 2)$; ≈ 0 means an absolute value less than 10^{-15} .

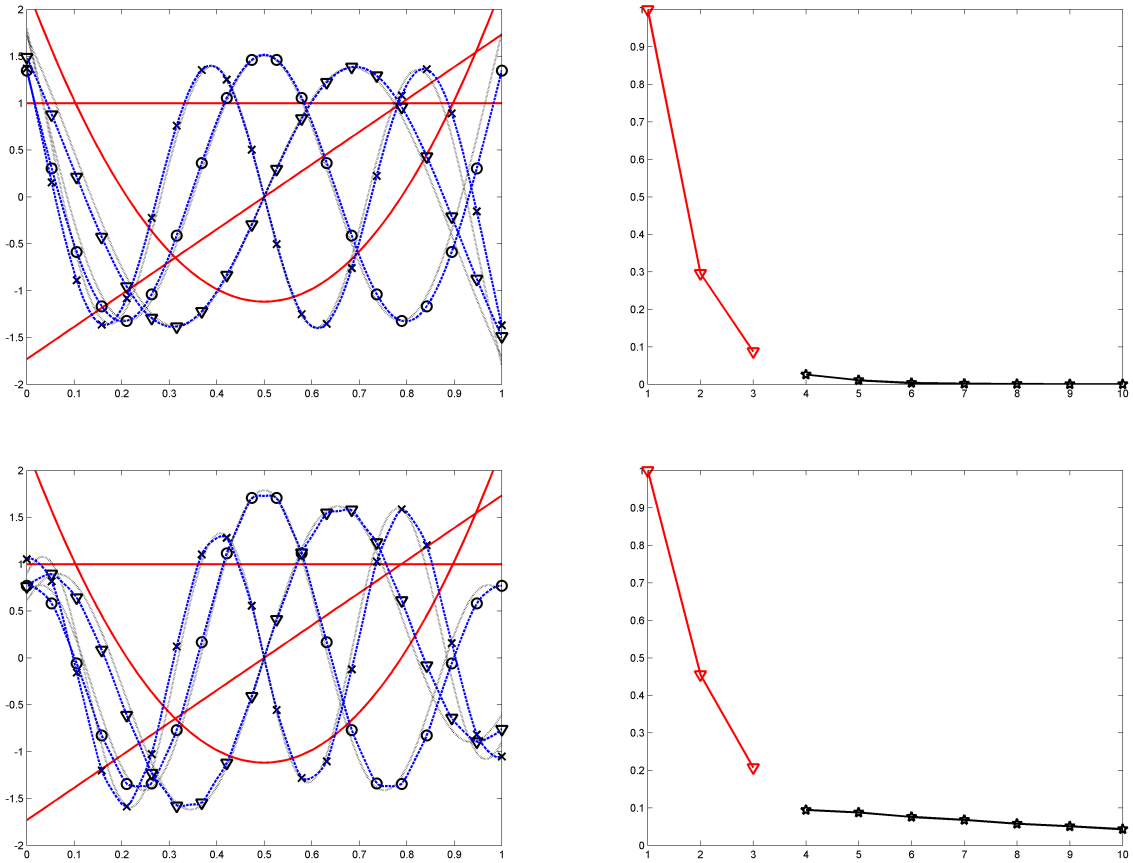


Figure 1: First eigenfunctions (left) and eigenvalues (right) for the univariate model with uniform measure on $[0, 1]$ and Matérn covariance $K_{3/2}(\cdot, \cdot; \theta)$, for $\theta = 2$ (top) and $\theta = 20$ (bottom).

see (3.9). A value of θ such that $\rho(\theta)$ is close to one then seems reasonable. For instance, when $q_1 = 100$, $n = 64$ and $p_i = 2$ for all i , we obtain here $\rho(2) \simeq 0.9993$ and $\rho(20) \simeq 0.8290$ for

$d = 2$, and $\rho(2) \simeq 0.9845$ and $\rho(20) \simeq 0.5083$ for $d = 3$, suggesting that 64 evaluations of a function of three variables may not be enough to reproduce its behaviour with a tensorised model based on Matérn 3/2 covariance with $\theta = 20$ and second-degree polynomials in each variable. The posterior distributions of the model parameters $\beta_{\underline{\ell}}$ and Sobol' indices depend on θ and rely on strong assumptions on the underlying model; they should thus be taken with caution. As Section 7 will illustrate, they can, however, be used as guidelines for designing experiments adapted to the estimation of Sobol' indices.

Remark 4.5. Although a rule based on the value of $\rho(\theta)$ could also be applied when different covariance functions $K_i(\cdot, \cdot; \theta_i)$ are used for different input variables, the choice of $\theta = (\theta_1, \dots, \theta_d)$ may quickly become cumbersome. On the other hand, when no prior information on $\mathbf{f}(\cdot)$ is available, it makes sense to take the same covariance and correlation length for all dimensions; see the examples in Section 7. Another option, which we shall not develop in this paper due to space-limitation, is to estimate θ from the data, by maximum likelihood or cross validation, in another (simpler) tensor-product model, prior to the eigendecomposition. For instance, when $p_i = 0$ for all i and all $K_i(\cdot, \cdot)$ coincide, we can estimate covariance parameters θ in a RF model with unknown mean and covariance

$$K^{(a)}(\mathbf{x}, \mathbf{y}; \theta) = \prod_{i=1}^d K_i(x_i, y_i; \theta), \quad \text{or} \quad K^{(b)}(\mathbf{x}, \mathbf{y}; \theta) = \prod_{i=1}^d [1 + \tilde{K}_i(x_i, y_i; \theta)], \quad (4.8)$$

see [9]. An example is presented in Section 7.1. \triangleleft

The Matérn 5/2 covariance function, $K_{5/2}(x, y; \theta) = (1 + \sqrt{5}\theta|x-y| + 5\theta^2|x-y|^2/3) \exp(-\sqrt{5}\theta|x-y|)$, with the same values of θ as above, yields plots hardly distinguishable from those presented in Figure 1. Similar experiments with other covariance functions confirm the intuition that the choice of the kernel among a class of smooth enough stationary kernels has little influence when considering only a few terms of the eigendecomposition. Note that once evaluations of $\mathbf{f}(\cdot)$ have been obtained, one can easily repeat estimations of Sobol' indices for different covariance kernels (using various smoothness assumptions and/or correlation lengths), different values of q_i and N , etc., thereby assessing the impact of these choices on the estimation.

Suppose now that $d = 2$, with $\mu_1 = \mu_2$ uniform on $[0, 1]$, and consider the tensorised model (3.10). We take $p_1 = p_2 = 2$ and use the covariance $K_{3/2}(x, y; 2)$ in each dimension, with the 100-point quadrature approximation $\hat{\mu}_1(100)$. For $N = 25$, the truncation set \mathbb{L}_N defined by (4.5) is equal to

$$\mathbb{L}_{25} = \left\{ \begin{array}{cccccccccccccccccccc} 0 & 0 & 1 & 1 & 0 & 2 & 1 & 2 & 0 & 3 & 0 & 4 & 2 & 1 & 3 & 0 & 5 & 1 & 4 & 2 & 3 & 0 & 6 & 1 & 5 \\ 0 & 1 & 0 & 1 & 2 & 0 & 2 & 1 & 3 & 0 & 4 & 0 & 2 & 3 & 1 & 5 & 0 & 4 & 1 & 3 & 2 & 6 & 0 & 5 & 1 \end{array} \right\}$$

The corresponding values of (log of) $\Lambda_{\underline{\ell}}$ are shown in Figure 2, see (4.6). The construction of the ϑ_{i, ℓ_i} in Section 4.3 implies that $\lambda_{1, \ell} \lambda_{2, \ell'} = \gamma_{1,1}^{(\ell+\ell')/3}$ for $\ell, \ell' \in \{0, \dots, 3\}$, which explains the presence of two triples and a quadruple of identical $\Lambda_{\underline{\ell}}$; pairs of identical values are simply due to an exchange between dimension indices, i.e., $\lambda_{1, \ell} \lambda_{2, \ell'} = \lambda_{2, \ell} \lambda_{1, \ell'}$.

Besides the 9 polynomial components $P_{1, \ell}(x_1)P_{2, \ell'}(x_2)$, $\ell, \ell' \in \{0, 1, 2\}$, the model (3.10) with $\mathbb{L} = \mathbb{L}_{25}$ also contains 16 components that involve (canonical extensions of) eigenfunctions $\varphi'_{i,j}(\cdot)$, for $i = 1, 2$ and $j \in \{1, \dots, 6\}$. Increasing N in \mathbb{L}_N allows modelling thinner details in the behaviour of $\mathbf{f}(\cdot)$, but this more precise modelling calls for a larger number of observations. This is why we suggest to choose N of the same order of magnitude as the projected number of evaluations of $\mathbf{f}(\cdot)$.

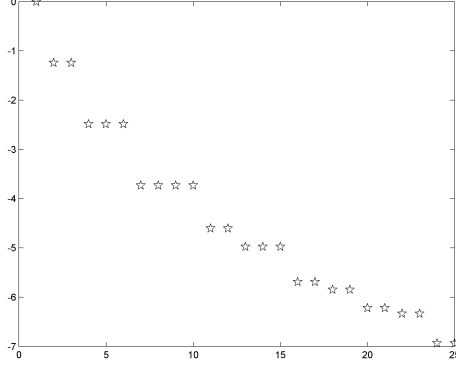


Figure 2: Eigenvalues $\Lambda_{\underline{\ell}}$ (log scale) in the tensorised model.

5 Estimation of Sobol' indices and credible intervals

Suppose that n evaluations of $f(\cdot)$ at $\mathcal{D}_n = \{\mathbf{x}_1, \dots, \mathbf{x}_n\} \subset \mathcal{X}^n$ have been performed, and denote

$$\mathbf{Y}_n = [f(\mathbf{x}_1), \dots, f(\mathbf{x}_n)]^T.$$

Also, in the BLM (3.10) with $\mathbb{L} = \mathbb{L}_N$ given by (4.5), denote $\mathbf{\Lambda} = \text{diag}\{\Lambda_{\underline{\ell}_k}, k = 1, \dots, M\}$, $\mathbf{\Psi}_n$ the $n \times M$ matrix with j, k term $\psi_{\underline{\ell}_k}(\mathbf{x}_j)$, for $j = 1, \dots, n$, $k = 1, \dots, M$, and $\mathbf{\Sigma}_n = \text{diag}\{s^2(\mathbf{x}_j), j = 1, \dots, n\}$ with $s^2(\mathbf{x})$ given by (3.11). The parameters $\boldsymbol{\beta} = (\beta_{\underline{\ell}_1}, \dots, \beta_{\underline{\ell}_M})^T$ have the normal prior $\mathcal{N}(\mathbf{0}, \sigma^2 \mathbf{\Lambda})$ and the errors $\boldsymbol{\epsilon}'_n = [\epsilon'(\mathbf{x}_1), \dots, \epsilon'(\mathbf{x}_n)]$ are normally distributed $\mathcal{N}(\mathbf{0}, \sigma^2 \mathbf{\Sigma}_n)$, see Section 4.3. However, the introduction of a prior on the trend parameters in Section 3.2 was only motivated by the construction of the tensorised model, and when estimating $\boldsymbol{\beta}$ we shall put an improper prior on the $\beta_{\underline{\ell}_k}$ that correspond to pure trend components in (3.10); that is, we set $\Lambda_{\underline{\ell}_k}^{-1} = 0$ for all k such that $\ell_{k,i} \leq p_i$ for all $i = 1, \dots, d$. We denote by $\mathbf{\Lambda}_0$ the corresponding diagonal matrix (it will only appear through its inverse, which is always finite). We also denote by \mathbb{K} the set of such k , with $|\mathbb{K}| = K$, and $\mathbf{\Lambda}' = \text{diag}\{\Lambda_{\underline{\ell}_k} : k \in \{1, \dots, M\} \setminus \mathbb{K}\}$; \mathbf{R}_n is the matrix formed by the columns of $\mathbf{\Psi}_n$ with indices in \mathbb{K} and $\mathbf{\Psi}'_n$ is formed by the remaining columns to $\mathbf{\Psi}_n$; $\boldsymbol{\alpha}$ is formed by the K components of $\boldsymbol{\beta}$ with indices in \mathbb{K} and $\boldsymbol{\beta}'$ by the other components of $\boldsymbol{\beta}$, having the prior distribution $\mathcal{N}(\mathbf{0}, \sigma^2 \mathbf{\Lambda}')$.

5.1 Estimation of indices

We estimate $\boldsymbol{\beta}$ by its posterior mean

$$\hat{\boldsymbol{\beta}}^n = \mathbf{M}_n^{-1} \mathbf{\Psi}_n^T \mathbf{\Sigma}_n^{-1} \mathbf{Y}_n,$$

with \mathbf{M}_n the Bayesian information matrix

$$\mathbf{M}_n = \mathbf{\Psi}_n^T \mathbf{\Sigma}_n^{-1} \mathbf{\Psi}_n + \mathbf{\Lambda}_0^{-1}. \quad (5.1)$$

Note that when the data $\{\mathbf{x}_k, f(\mathbf{x}_k)\}$ arrive sequentially, classical recursive least squares formulae can be used to avoid repetitions of matrix inversion. Following the developments in Section 2.2, for any index set $\mathcal{U} \subset \{1, \dots, d\}$ we estimate $\underline{S}_{\mathcal{U}}$, defined in (2.3), by

$$\hat{\underline{S}}_{\mathcal{U}}^n = \frac{\sum_{\underline{\ell} \in \mathbb{L}_N(\mathcal{U})} (\hat{\beta}_{\underline{\ell}}^n)^2}{\sum_{\underline{\ell} \in \mathbb{L}_N^*} (\hat{\beta}_{\underline{\ell}}^n)^2}, \quad (5.2)$$

where $\mathbb{L}_N^* = \{\underline{\ell}_k \in \mathbb{L}_N : \underline{\ell}_k \neq \mathbf{0}\} = \{\underline{\ell}_2, \dots, \underline{\ell}_M\}$ and $\mathbb{L}_N(\mathcal{U}) = \{\underline{\ell}_k \in \mathbb{L}_N^* : \ell_{k,i} = 0 \text{ for all } i \notin \mathcal{U}\}$, with \mathbb{L}_N given by (4.5). This allows us to estimate all Sobol' indices $S_{\mathcal{V}}$ and $\bar{S}_{\mathcal{V}}$ for any index set \mathcal{V} , see Section 2. Any such estimate has the form

$$\hat{S}^n = \frac{\sum_{\underline{\ell}_k \in \tilde{\mathbb{L}}_N} (\hat{\beta}_{\underline{\ell}_k}^n)^2}{\sum_{k=2}^M (\hat{\beta}_{\underline{\ell}_k}^n)^2},$$

for some subset $\tilde{\mathbb{L}}_N$ of \mathbb{L}_N^* , and is thus given by the ratio of two (simple) quadratic forms in $\hat{\beta}^n$. Note that \hat{S}^n does not depend on the value of σ^2 .

5.2 Estimation of σ^2

The marginal distribution of \mathbf{Y}_n given $\boldsymbol{\alpha}$ and σ^2 is normal $\mathcal{N}(\mathbf{R}_n \boldsymbol{\alpha}, \sigma^2(\boldsymbol{\Sigma}_n + \boldsymbol{\Psi}'_n \boldsymbol{\Lambda}' \boldsymbol{\Psi}_n'^T))$. With an improper prior on σ^2 (with density proportional to $1/\sigma^2$), its posterior distribution is inverse chi-square with $n - K$ degrees of freedom and such that $\mathbb{E}\{1/\sigma^2 | \mathbf{Y}_n\} = 1/\hat{\sigma}_n^2$, with

$$\hat{\sigma}_n^2 = \frac{1}{n - K} (\mathbf{Y}_n - \mathbf{R}_n \hat{\boldsymbol{\alpha}}^n)^T (\boldsymbol{\Sigma}_n + \boldsymbol{\Psi}'_n \boldsymbol{\Lambda}' \boldsymbol{\Psi}_n'^T)^{-1} (\mathbf{Y}_n - \mathbf{R}_n \hat{\boldsymbol{\alpha}}^n)$$

(the restricted maximum likelihood estimator; see [34, p. 170]), where $\hat{\boldsymbol{\alpha}}^n$ corresponds to the K components of $\hat{\beta}^n$ with indices in \mathbb{K} .

Given σ^2 , the posterior distribution $\pi(\boldsymbol{\beta} | \mathbf{Y}_n, \sigma^2)$ of $\boldsymbol{\beta}$ is normal $\mathcal{N}(\hat{\beta}^n, \sigma^2 \mathbf{M}_n^{-1})$, with \mathbf{M}_n given by (5.1). When the number of degrees of freedom, $n - K$, of the posterior distribution of σ^2 is large enough (note that $K = 1$ when all p_i equal zero, see Section 4.5), we may consider that the posterior $\pi(\boldsymbol{\beta} | \mathbf{Y}_n)$ is normal $\mathcal{N}(\hat{\beta}^n, \hat{\sigma}_n^2 \mathbf{M}_n^{-1})$, and we shall make this approximation in the following.

5.3 Distribution of Sobol' indices

Take any index given by

$$S_{\tilde{\mathbb{L}}_N}(\boldsymbol{\beta}) = \frac{\sum_{\underline{\ell}_k \in \tilde{\mathbb{L}}_N} \beta_{\underline{\ell}_k}^2}{\sum_{k=2}^M \beta_{\underline{\ell}_k}^2} \quad (5.3)$$

for some $\tilde{\mathbb{L}}_N \subseteq \mathbb{L}_N^*$ (which is well defined when $\beta_{\underline{\ell}_k} \neq 0$ for at least one $k > 1$). We consider two different approximations of its posterior distribution.

Remark 5.1. The value of $S_{\tilde{\mathbb{L}}_N}(\boldsymbol{\beta})$ is invariant by a scale transformation of the $\beta_{\underline{\ell}_k}$, with the consequence that when $\boldsymbol{\beta}$ has the normal prior $\mathcal{N}(\mathbf{0}, \sigma^2 \boldsymbol{\Lambda})$, the prior distribution of $S_{\tilde{\mathbb{L}}_N}(\boldsymbol{\beta})$ does not depend on the value of σ^2 . \triangleleft

5.3.1 Normal approximation

Consider the ratio (5.3). Since $\boldsymbol{\beta}$ has the normal posterior $\mathcal{N}(\hat{\beta}^n, \hat{\sigma}_n^2 \mathbf{M}_n^{-1})$, we approximate the posterior distribution $\pi(S_{\tilde{\mathbb{L}}_N}(\boldsymbol{\beta}) | \mathbf{Y}_n)$ by the normal distribution with mean $S_{\tilde{\mathbb{L}}_N}(\hat{\beta}^n)$ and variance

$$V_{\tilde{\mathbb{L}}_N}^n = \hat{\sigma}_n^2 \left. \frac{\partial S_{\tilde{\mathbb{L}}_N}(\boldsymbol{\beta})}{\partial \boldsymbol{\beta}^T} \right|_{\hat{\beta}^n} \mathbf{M}_n^{-1} \left. \frac{\partial S_{\tilde{\mathbb{L}}_N}(\boldsymbol{\beta})}{\partial \boldsymbol{\beta}} \right|_{\hat{\beta}^n}.$$

Direct calculation gives

$$\frac{\partial S_{\tilde{\mathbb{L}}_N}(\boldsymbol{\beta})}{\partial \boldsymbol{\beta}} = \frac{2}{\boldsymbol{\beta}^T \mathbf{J} \boldsymbol{\beta}} \boldsymbol{\Delta}_{\tilde{\mathbb{L}}_N} \boldsymbol{\beta}, \quad (5.4)$$

with $\mathbf{\Delta}_{\tilde{\mathbb{L}}_N}$ the diagonal matrix

$$\mathbf{\Delta}_{\tilde{\mathbb{L}}_N} = \mathbf{U}_{\tilde{\mathbb{L}}_N} - S_{\tilde{\mathbb{L}}_N} \mathbf{J}, \quad (5.5)$$

where $\mathbf{U}_{\tilde{\mathbb{L}}_N} = \text{diag}\{u_{\ell_k}, k = 1, \dots, M\}$, $u_{\ell_k} = 1$ if $\ell_k \in \tilde{\mathbb{L}}_N$ and is zero otherwise, and \mathbf{J} is the $M \times M$ diagonal matrix $\text{diag}\{0, 1, \dots, 1\}$. We thus obtain

$$V_{\tilde{\mathbb{L}}_N}^n = \frac{4\hat{\sigma}_n^2}{[(\hat{\boldsymbol{\beta}}^n)^T \mathbf{J} \hat{\boldsymbol{\beta}}^n]^2} (\hat{\boldsymbol{\beta}}^n)^T \mathbf{\Delta}_{\tilde{\mathbb{L}}_N} \mathbf{M}_n^{-1} \mathbf{\Delta}_{\tilde{\mathbb{L}}_N} \hat{\boldsymbol{\beta}}^n. \quad (5.6)$$

Critical values for the normal distribution $\mathcal{N}(S_{\tilde{\mathbb{L}}_N}(\hat{\boldsymbol{\beta}}^n), V_{\tilde{\mathbb{L}}_N}^n)$, truncated to $[0, 1]$, provide approximate credible intervals for $S_{\tilde{\mathbb{L}}_N}(\boldsymbol{\beta})$. Notice that the estimation of $S_{\tilde{\mathbb{L}}_N}(\boldsymbol{\beta})$ and the construction of these credible intervals can be data-recursive; see also [15, 16] for another data-recursive approach for first and second-order indices.

5.3.2 Exact posterior distribution of Sobol' indices for normal parameters

We use the results in [19] and [4] to derive the exact distribution of $S_{\tilde{\mathbb{L}}_N}(\boldsymbol{\beta})$ defined by (5.3) when $\boldsymbol{\beta}$ is normal $\mathcal{N}(\hat{\boldsymbol{\beta}}^n, \hat{\sigma}_n^2 \mathbf{M}_n^{-1})$. Denoting $\mathbf{A} = \hat{\sigma}_n^2 \mathbf{M}_n^{-1/2} \mathbf{U}_{\tilde{\mathbb{L}}_N} \mathbf{M}_n^{-1/2}$ and $\mathbf{B} = \hat{\sigma}_n^2 \mathbf{M}_n^{-1/2} \mathbf{J} \mathbf{M}_n^{-1/2}$, we get

$$\mathbb{F}_{\tilde{\mathbb{L}}_N}(r) = \text{Prob}\{S_{\tilde{\mathbb{L}}_N}(\boldsymbol{\beta}) \leq r\} = \text{Prob}\{\mathbf{t}^T (\mathbf{A} - r\mathbf{B}) \mathbf{t} \leq 0\},$$

where $\mathbf{t} \sim \mathcal{N}(\mathbf{0}, \mathbf{I}_M)$. Next, we construct the spectral decomposition $\mathbf{A} - r\mathbf{B} = \mathbf{P} \mathbf{D} \mathbf{P}^T$, with $\mathbf{D} = \text{diag}\{\delta_1, \dots, \delta_M\}$, and compute $\boldsymbol{\omega} = (\omega_1, \dots, \omega_M)^T = \hat{\sigma}_n^{-1} \mathbf{P}^T \mathbf{M}_n^{1/2} \hat{\boldsymbol{\beta}}^n$. Then,

$$\mathbb{F}_{\tilde{\mathbb{L}}_N}(r) = \frac{1}{2} - \frac{1}{\pi} \int_0^\infty \frac{\sin \beta(u)}{u \gamma(u)} du, \quad (5.7)$$

where

$$\beta(u) = \frac{1}{2} \sum_{k=1}^M \left[\arctan(\delta_k u) + \frac{\omega_k^2 \delta_k u}{1 + \delta_k^2 u^2} \right] \quad \text{and} \quad \gamma(u) = \exp \left\{ \frac{1}{2} \sum_{k=1}^M \left[\frac{\omega_k^2 \delta_k^2 u^2}{1 + \delta_k^2 u^2} + \frac{1}{2} \log(1 + \delta_k^2 u^2) \right] \right\};$$

see [19]. The density of $S_{\tilde{\mathbb{L}}_N}(\boldsymbol{\beta})$ is given by

$$f_{\tilde{\mathbb{L}}_N}(r) = \frac{1}{\pi} \int_0^\infty \frac{\rho(u) \cos \beta(u) - u \delta(u) \sin \beta(u)}{2\gamma(u)} du, \quad (5.8)$$

where $\beta(u)$ and $\gamma(u)$ are defined above and

$$\rho(u) = \text{trace}[\mathbf{H} \mathbf{F}^{-1}] + \boldsymbol{\omega}^T \mathbf{F}^{-1} (\mathbf{H} - u^2 \mathbf{D} \mathbf{H} \mathbf{D}) \mathbf{F}^{-1} \boldsymbol{\omega}, \quad \delta(u) = \text{trace}[\mathbf{H} \mathbf{D} \mathbf{F}^{-1}] + 2 \boldsymbol{\omega}^T \mathbf{F}^{-1} \mathbf{H} \mathbf{D} \mathbf{F}^{-1} \boldsymbol{\omega},$$

with $\mathbf{H} = \mathbf{P}^T \mathbf{B} \mathbf{P}$ and $\mathbf{F} = \mathbf{I}_M + u^2 \mathbf{D}^2$; see [4].

Using the expressions (5.7) and (5.8) of $\mathbb{F}_{\tilde{\mathbb{L}}_N}(r)$ and $f_{\tilde{\mathbb{L}}_N}(r)$, we can easily construct credible intervals of minimum length for $S_{\tilde{\mathbb{L}}_N}(\boldsymbol{\beta})$, e.g. via dichotomy search. For a given $\alpha \in (0, 1)$, e.g., $\alpha = 0.05$, we find $b \in [0, 1]$ such that $\mathbb{F}_{\tilde{\mathbb{L}}_N}(b) - \mathbb{F}_{\tilde{\mathbb{L}}_N}[a(b)] = 1 - \alpha$, where $a(b) < b$ is such that $f_{\tilde{\mathbb{L}}_N}[a(b)] = f_{\tilde{\mathbb{L}}_N}(b)$ and is also determined by dichotomy search. An illustration is given in Figure 4-left. Of course, the required integral computations make this construction significantly heavier than the derivation of approximate intervals based on the normal approximation of Section 5.3.1.

6 Experimental design

We consider the usual situation where we want to simultaneously estimate J different indices $\mathbf{S}_{\tilde{\mathbb{L}}_{N,1,\dots,J}}(\boldsymbol{\beta}) = (S_{\tilde{\mathbb{L}}_{N,1}}(\boldsymbol{\beta}), \dots, S_{\tilde{\mathbb{L}}_{N,J}}(\boldsymbol{\beta}))^T$ corresponding to different sets $\tilde{\mathbb{L}}_{N,j} = \tilde{\mathbb{L}}_N(\mathcal{U}_j)$ in (5.3). For instance, to estimate the d first-order total indices \bar{S}_i , $i = 1, \dots, d$, we should consider the d sets $\tilde{\mathbb{L}}_{N,i} = \{\ell_k \in \mathbb{L}_N^* : \ell_{k,i} \neq 0\}$; see Section 2.2. Denote by $\mathbf{V}(\boldsymbol{\beta})$ the $M \times J$ matrix formed from the derivatives (5.4) of the J indices of interest,

$$\mathbf{V}(\boldsymbol{\beta}) = \frac{2}{\boldsymbol{\beta}^T \mathbf{J} \boldsymbol{\beta}} \left[\boldsymbol{\Delta}_{\tilde{\mathbb{L}}_{N,1}} \boldsymbol{\beta} \mid \dots \mid \boldsymbol{\Delta}_{\tilde{\mathbb{L}}_{N,J}} \boldsymbol{\beta} \right]. \quad (6.1)$$

Following developments similar to those in Section 5.3.1, we can approximate the posterior joint distribution of $S_{\tilde{\mathbb{L}}_{N,1}}, \dots, S_{\tilde{\mathbb{L}}_{N,J}}$ by the normal distribution $\mathcal{N}(\mathbf{S}_{\tilde{\mathbb{L}}_{N,1,\dots,J}}(\hat{\boldsymbol{\beta}}^n), \hat{\sigma}_n^2 \boldsymbol{\Omega}_n(\boldsymbol{\beta}^n))$, with $\boldsymbol{\Omega}_n(\boldsymbol{\beta})$ the $J \times J$ matrix

$$\boldsymbol{\Omega}_n(\boldsymbol{\beta}) = \mathbf{V}^T(\boldsymbol{\beta}) \mathbf{M}_n^{-1} \mathbf{V}(\boldsymbol{\beta}),$$

and construct experimental designs \mathcal{D}_n that minimise a scalar function of $\boldsymbol{\Omega}_n$. We suppose that $\mathcal{D}_n \subset \mathcal{X}_Q = \{\mathbf{x}^{(1)}, \dots, \mathbf{x}^{(Q)}\}$, a given finite set of candidate points; for instance, \mathcal{X}_Q may be given by the first Q points of a low discrepancy sequence in \mathcal{X} . Notice that it is computationally advantageous to compute all $\phi'_i(\{\mathbf{x}^{(j)}\}_i)$ given by (4.2) and all $K'_i(\{\mathbf{x}^{(j)}\}_i, \{\mathbf{x}^{(j)}\}_i)$ given by (4.3) in advance, for $j = 1, \dots, Q$ and $i = 1, \dots, d$. We only present the construction of adaptive designs; optimal (non-adaptive) designs are briefly considered in the Appendix.

The choice of suitable design criteria depends on which aspect of precision we consider more appealing. Assuming that the indices of interest are approximately normally distributed, the D-optimality criterion $\det(\boldsymbol{\Omega}_n)$ is related to the (squared) volume of joint confidence ellipsoids; the A-optimality criterion $\text{trace}(\boldsymbol{\Omega}_n)$ is related to the sum of squared lengths of the principal axes of these ellipsoids; the MV-optimality criterion $\max[\text{diag}(\boldsymbol{\Omega}_n)]$ is related to the maximum of the variances of individual indices, see [21].

D-optimality for the estimation of first-order Sobol' indices in PCE models is considered in [5], and we follow the same line in the more general framework considered here. We suppose that n_0 evaluations of $\mathbf{f}(\cdot)$ have been performed, such that \mathbf{M}_{n_0} is nonsingular. Then, for each $n \geq n_0$, after estimation of $\hat{\boldsymbol{\beta}}^n$ from n evaluations of $\mathbf{f}(\cdot)$, we choose the next design point \mathbf{x}_{n+1} that yields the largest decrease of $\mathcal{C}[\boldsymbol{\Omega}_{n+1}(\hat{\boldsymbol{\beta}}^n)]$, with $\mathcal{C}(\cdot)$ one of the criteria above.

Straightforward calculations indicate that

$$\mathbf{x}_{n+1} \in \text{Arg max}_{\mathbf{x} \in \mathcal{X}_Q} \frac{\boldsymbol{\psi}^T(\mathbf{x}) \mathbf{M}_n^{-1} \mathbf{V}(\hat{\boldsymbol{\beta}}^n) [\mathbf{V}^T(\hat{\boldsymbol{\beta}}^n) \mathbf{M}_n^{-1} \mathbf{V}(\hat{\boldsymbol{\beta}}^n)]^{-1} \mathbf{V}^T(\hat{\boldsymbol{\beta}}^n) \mathbf{M}_n^{-1} \boldsymbol{\psi}(\mathbf{x})}{s^2(\mathbf{x}) + \boldsymbol{\psi}^T(\mathbf{x}) \mathbf{M}_n^{-1} \boldsymbol{\psi}(\mathbf{x})} \quad (6.2)$$

when minimising $\det[\boldsymbol{\Omega}_{n+1}(\hat{\boldsymbol{\beta}}^n)]$,

$$\mathbf{x}_{n+1} \in \text{Arg max}_{\mathbf{x} \in \mathcal{X}_Q} \frac{\boldsymbol{\psi}^T(\mathbf{x}) \mathbf{M}_n^{-1} \mathbf{V}(\hat{\boldsymbol{\beta}}^n) \mathbf{V}^T(\hat{\boldsymbol{\beta}}^n) \mathbf{M}_n^{-1} \boldsymbol{\psi}(\mathbf{x})}{s^2(\mathbf{x}) + \boldsymbol{\psi}^T(\mathbf{x}) \mathbf{M}_n^{-1} \boldsymbol{\psi}(\mathbf{x})} \quad (6.3)$$

when minimising $\text{trace}[\boldsymbol{\Omega}_{n+1}(\hat{\boldsymbol{\beta}}^n)]$, and

$$\mathbf{x}_{n+1} \in \text{Arg max}_{\mathbf{x} \in \mathcal{X}_Q} \min_{j=1,\dots,J} \left\{ \frac{[\boldsymbol{\psi}^T(\mathbf{x}) \mathbf{M}_n^{-1} \mathbf{V}(\hat{\boldsymbol{\beta}}^n) \mathbf{e}_j]^2}{s^2(\mathbf{x}) + \boldsymbol{\psi}^T(\mathbf{x}) \mathbf{M}_n^{-1} \boldsymbol{\psi}(\mathbf{x})} - \mathbf{e}_j^T \mathbf{V}^T(\hat{\boldsymbol{\beta}}^n) \mathbf{M}_n^{-1} \mathbf{V}(\hat{\boldsymbol{\beta}}^n) \mathbf{e}_j \right\} \quad (6.4)$$

when minimising $\max\{\text{diag}[\boldsymbol{\Omega}_{n+1}(\hat{\boldsymbol{\beta}}^n)]\}$, with $\boldsymbol{\psi}(\mathbf{x}) = [\psi_{\ell_1}(\mathbf{x}), \dots, \psi_{\ell_M}(\mathbf{x})]^T$ and \mathbf{e}_j the j th canonical basis vector of \mathbb{R}^J (any of the maximisers can be chosen for \mathbf{x}_{n+1} in case there are several). Weighed versions of $\text{trace}(\boldsymbol{\Omega})$ and $\max[\text{diag}(\boldsymbol{\Omega})]$ might also be considered, for instance in order to consider individual relative precision of the J indices, by introducing weights along $\text{diag}(\boldsymbol{\Omega})$.

Remark 6.1. The presence of independent errors in the model (3.10) has the consequence that the sequential construction above may yield repetitions of observations at the same design point. When this happens, it may be interpreted as an indication that the approximations involved are too rough for the number of observations considered and should be refined by (i) considering a finer set \mathcal{X}_Q and/or (ii) enlarging the number of components in (3.10), that is, the value of N in (4.5); see Figure 11 for an illustration. Note that repetitions can always be avoided by considering that $s^2(\mathbf{x})$ is infinite for any \mathbf{x} already selected. \triangleleft

7 Numerical examples

7.1 Ishigami function

This function depends on three variables and is frequently used as a test-case in sensitivity analysis. It is given by $f(\mathbf{x}) = \sin(x_1) + a \sin^2(x_2) + b x_3^4 \sin(x_1)$, \mathbf{x} being uniformly distributed in $\mathcal{X} = [-\pi, \pi]^3$. We shall use the values $a = 7$ and $b = 0.1$. The first-order indices are equal to

$$S_1 = (b\pi^4/5 + b^2\pi^8/50 + 1/2)/\Delta, \quad S_2 = a^2/(8\Delta), \quad S_3 = 0$$

where $\Delta = a^2/8 + b\pi^4/5 + b^2\pi^8/18 + 1/2$, the second-order indices are all zero excepted $S_{1,3} = 8b^2\pi^8/(225\Delta)$. We have, by definition, see Section 2.1,

$$\bar{S}_1 = S_1 + S_{1,3}, \quad \bar{S}_2 = S_2, \quad \bar{S}_3 = S_{1,3}, \quad \underline{S}_{1,2} = S_1 + S_2, \quad \underline{S}_{1,3} = S_{1,3} + S_1 \text{ and } \underline{S}_{2,3} = S_2.$$

We approximate each marginal of μ by the discrete uniform measure that puts weight $1/100$ at each of the points $(j-1)/99$, $j = 1, \dots, q = 100$, and use the covariance $K_{3/2}(x, y; \theta)$, see Section 4.6. We set $p_i = 0$ for $i = 1, 2, 3$ (we have observed that the performances are significantly deteriorated when setting the polynomial degrees p_i to positive values). We estimate the indices by evaluating $f(\cdot)$ at the first n points of Sobol' low-discrepancy sequence in $[0, 1]^3$, and take $N = n$ in (4.5).

Figure 3-left shows the density (5.8) of the prior distribution of first-order indices S_i (the same for $i = 1, 2, 3$) for $\theta = 2$ (solid line) and $\theta = 20$ (dashed line). Figure 3-right shows the two posterior distributions obtained for S_1 when $n = 64$, $\theta = 2$ (solid line) and $\theta = 20$ (dashed line), β having the normal distribution $\mathcal{N}(\hat{\beta}^n, \hat{\sigma}_n^2 \mathbf{M}_n^{-1})$; see Section 5.3.2. The true value of S_1 is indicated by a star. The model with $\theta = 2$ seems able to adequately capture the global behaviour of $f(\cdot)$, whereas prior weights on components with fast variations are exaggeratedly large when $\theta = 20$, see the discussion in Section 4.6, which renders the estimation less precise.

Figure 4-left shows the posterior density (5.8) for S_1 (solid line, same as in Figure 3-right), the minimum-length 95% credible interval, and the normal approximation of the posterior (dashed line), all for $\theta = 2$. The estimator (5.2) gives $\hat{S}_1^{64} \simeq 0.3337$, reasonably close to the true value $S_1 \simeq 0.3139$. Figure 4-right shows the posterior density (5.8) of $S_{1,2}$ (solid line) and its normal approximation (dashed line). Figure 5 presents the same information for $S_{1,3}$, when $n = 64$ (left) and $n = 256$ (right). The estimation of second-order indices is clearly more difficult: when $n = 64$, $S_{1,2}$ tends to be over-estimated (Figure 4-right) and $S_{1,3}$ underestimated (Figure 5-left). However, the situation improves when increasing n , with $\hat{S}_{1,2}^{256} \simeq 7.10^{-4}$ and $\hat{S}_{1,3}^{256} \simeq 0.2408$, see Figure 5-right. We obtain slightly better results when we first estimate θ in the RF model with unknown mean and covariance $K^{(a)}(\cdot, \cdot; \theta)$ in (4.8) from the same data, and then plug the estimated $\hat{\theta}^n$ into $K_i(\cdot, \cdot; \theta)$. Estimation of θ by leave-one-out cross validation, see [8], gives $\hat{\theta}_{LVO}^{64} \simeq 1.32$ and $\hat{S}_1^{64} \simeq 0.3188$; $\hat{\theta}_{LVO}^{256} \simeq 1.25$ and $\hat{S}_{1,2}^{256} \simeq 9.10^{-4}$, $\hat{S}_{1,3}^{256} \simeq 0.2448$. Estimating each θ_i separately in the covariance $\prod_{i=1}^3 K_i(x_i, y_i; \theta_i)$ does not improve performance; the results are slightly worse when estimating θ in

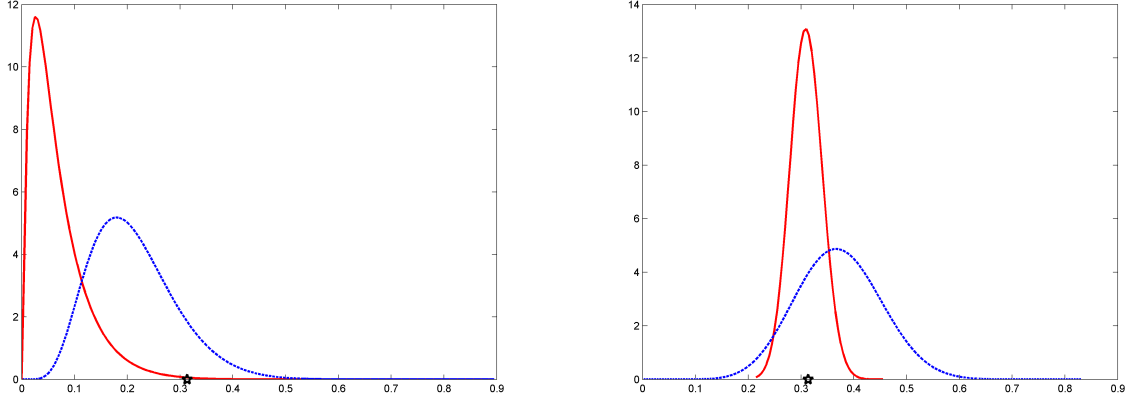


Figure 3: Ishigami function. Left: density (5.8) for S_i (first-order indices) when β has the prior distribution $\mathcal{N}(\mathbf{0}, \sigma^2 \mathbf{\Lambda})$ (see Remark 5.1). Right: density of S_1 when β has the posterior distribution $\mathcal{N}(\hat{\beta}^n, \hat{\sigma}_n^2 \mathbf{M}_n^{-1})$, $n = 64$. The covariance for univariate models is $K_{3/2}(x, y; 2)$ (red solid line) or $K_{3/2}(x, y; 20)$ (blue dashed line); $S_1 \simeq 0.3139$ is indicated by a star.

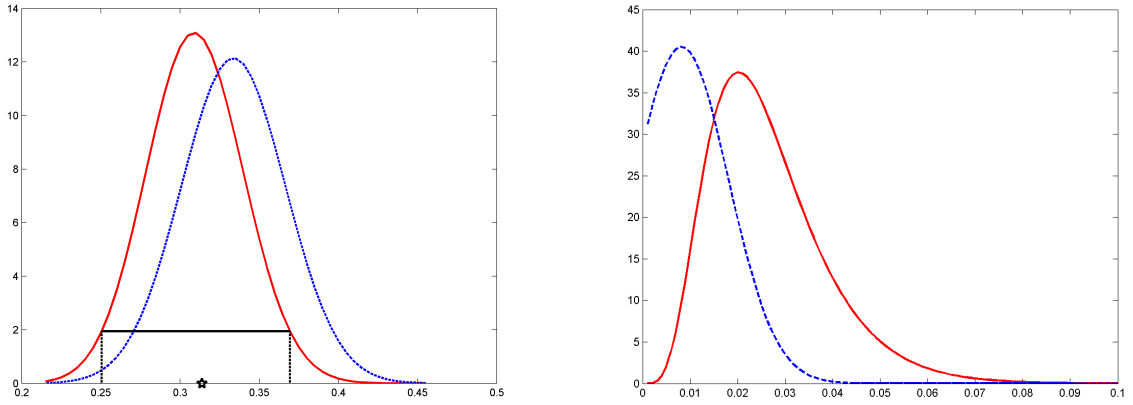


Figure 4: Ishigami function: posterior distributions for $n = 64$ with covariance $K_{3/2}(x, y; 2)$. Left: posterior density (5.8) for S_1 (red solid line) and minimum-length 95% credible interval; normal approximation (blue dashed line); $S_1 \simeq 0.3139$ (star). Right: posterior density (5.8) for $S_{1,2}$ (red solid line) and its normal approximation (blue dashed line); the true value is zero.

$K^{(b)}(\cdot, \cdot; \theta)$ compared with those for $\theta = 2$. Although this confirms the intuition that estimation of θ may improve performance, we shall always use $K_i(x, y) = K_{3/2}(x, y; 2)$ in the rest of the section.

Figure 6-left presents the evolution of the first order-index \hat{S}_1^n , see (5.2), with $\hat{\beta}^n$ estimated from evaluations at successive points of Sobol' sequence. After a batch of $n_0 = 10$ evaluations, we use a recursive construction for $\hat{\beta}^n$, and thus for \hat{S}_1^n , for $n = 11, \dots, 256$ (dashed line). The 95% credible intervals for the normal approximation (Section 5.3.1) are shown in dotted line; the true value of S_1 corresponds to the horizontal solid line. Figure 6-right presents the same information for S_2 (top) and S_3 (bottom). We have taken $N = 256$ in (4.5) and $p_i = 0$ for $i = 1, 2, 3$.

The function $f(\cdot)$ is fixed, but we may consider the variability of estimated indices when using

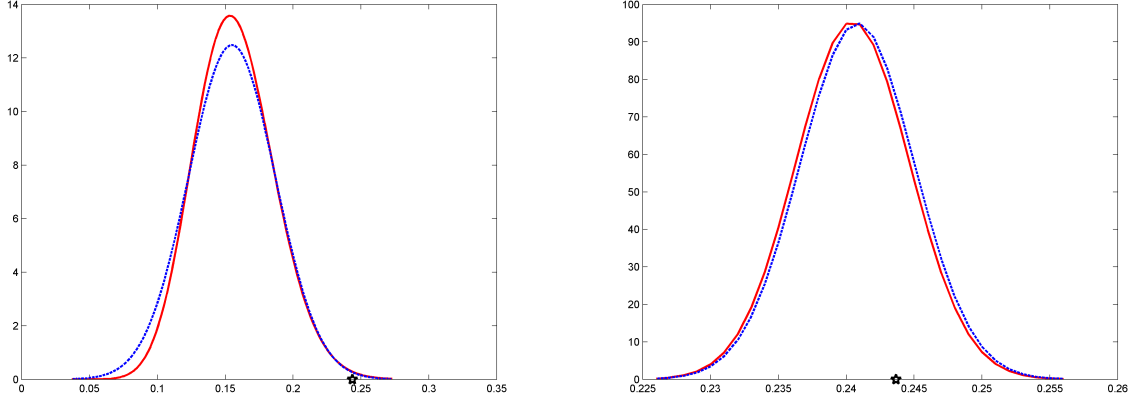


Figure 5: Ishigami function: posterior density (5.8) for $S_{1,3}$ (red solid line) and its normal approximation (blue dashed line) with covariance $K_{3/2}(x, y; 2)$. Left: $n = 64$; Right: $n = 256$; $S_{1,3} \simeq 0.2437$ is indicated by a star.

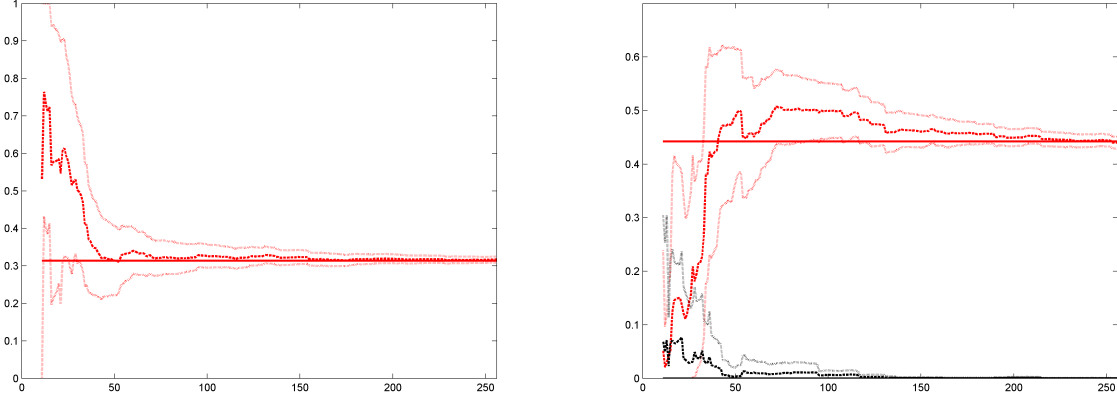


Figure 6: Ishigami function: estimated first-order indices (dashed line) and normal approximation of 95% credible intervals (dotted lines) with a tensorised BLM using $K_{3/2}(x, y; 2)$ and $N = 256$; the solid line indicates the true value. Left: S_1 ; right: S_2 (top) and S_3 (bottom).

different designs. We take $N = n$ in (4.5), $p_i = 0$ for all i and evaluate $\mathbf{f}(\cdot)$ at 100 different n -point Lh designs $\mathcal{D}_n^{(k)}$ constructed as follows. We first generate 10,000 random Lh designs in \mathcal{X} , and then select the 100 designs having the smallest value of $J_q(\cdot)$ defined by

$$J_q(\mathcal{D}_n) = \sum_{i=1}^n \min_{j \neq i} \|\mathbf{x}_j - \mathbf{x}_i\|^q, \quad q < 0,$$

with $\mathcal{D}_n = \{\mathbf{x}_1, \dots, \mathbf{x}_n\}$. $J_q^{1/q}(\mathcal{D}_n)$ tends to $J_{Mm}(\mathcal{D}_n) = \min_{i \neq j} \|\mathbf{x}_j - \mathbf{x}_i\|$ as q tends to $-\infty$, but its value depends on the respective positions of all points, contrary to the maximin criterion $J_{Mm}(\cdot)$. A design optimal for $J_q(\cdot)$ is $n^{1/q}$ -efficient for $J_{Mm}(\cdot)$ in the design family considered [27]; we take $q = -20$ to select designs having good space-filling properties. The left column

of Figure 7 presents box-plots (median, 25th and 75th percentiles and minimum and maximum values) of the errors $\hat{S}^n - S$, for $n = 64$ (top), 128 (middle) and 256 (bottom) respectively, for first-order, total, second-order and closed-second-order indices. We can see that the estimation is already reasonably accurate for small n (the results do not improve when we estimate θ by cross validation). Table 2 gives the empirical coverage probabilities (in %), for the 100 random Lh designs, of approximate 2σ credible intervals constructed with the variance $V_{\mathbb{L}_N}^n$ given by (5.6), for first-order indices (S_1, S_2, S_3) , total indices $(\bar{S}_1, \bar{S}_2, \bar{S}_3)$, second-order indices $(S_{1,2}, S_{1,3}, S_{2,3})$ and closed-second-order indices $(\underline{S}_{1,2}, \underline{S}_{1,3}, \underline{S}_{2,3})$. Although $V_{\mathbb{L}_N}^n$ accounts for uncertainty due to the possible variability of $f(\cdot)$ conditional on evaluations at a fixed design, by considering different designs of the same type (they are all space-filling and have the same one-dimensional projections) we try to mimic the behaviour of different $f(\cdot)$ for the same design. The coverage probabilities in Table 2 are acceptable in most cases. The small coverage probabilities observed for $S_{1,3}$ can be explained by the presence of a small estimation bias, see Figure 7, which may be related to the fact that the 100 designs considered are not particularly adapted to the estimation of indices. For the design used in Figure 6 (256 points of Sobol' sequence), we obtain $\hat{S}_{1,3}^{256} - S_{1,3} \simeq -0.0029$; for the design in Figure 9 (adaptive MV-optimal) we get $\hat{S}_{1,3}^{256} - S_{1,3} \simeq 0.0013$.

	S_i	\bar{S}_i	$S_{i,j}$	$\underline{S}_{i,j}$
$n = 64$	92	98	100	97
	98	99	67	99
	99	97	100	98
$n = 128$	100	93	99	78
	95	95	59	93
	97	78	96	93
$n = 256$	99	96	99	85
	97	96	73	96
	89	85	65	96

Table 2: Empirical coverage probabilities (in %), for 100 random Lh designs, of approximate 2σ credible intervals for (S_1, S_2, S_3) , $(\bar{S}_1, \bar{S}_2, \bar{S}_3)$, $(S_{1,2}, S_{1,3}, S_{2,3})$ and $(\underline{S}_{1,2}, \underline{S}_{1,3}, \underline{S}_{2,3})$ (BLM with $K_{3/2}(x, y; 2)$).

We now consider estimation of indices via (Legendre) polynomial-chaos expansion. When the total polynomial degree is D , the model contains $M = \binom{D+d}{d}$ parameters. Figure 8 presents the same information as Figure 6, using the same design points. We take $D = 5$, which gives a model with $M = 56$ parameters. We start with a batch of $n_0 = 64$ observations and then estimate $\hat{\beta}^n$ by recursive least-squares, for $n = 65, \dots, 256$. When the number of observations is small, we are over-confident in the model, although it is not flexible enough to estimate the indices correctly; when n increases, confidence in the model decreases due to a bad fitting with 56 tuning parameters only. Next, using the same random Lh designs as in Figure 7-left, we select the total degree D that gives the best estimation (which is possible here since we know the true value of indices). When $n = 64$ (128 and 256, respectively), this gives a model of degree 4 (6 and 8, respectively), with 35 (84 and 165, respectively) parameters. The results (box-plots) are presented in the right column of Figure 7. Although we have adapted the total degree of the model to the sample size (which is not an easy task in practice), comparison with the left column indicates that performance are significantly worse than with the tensorised BLM.

Finally; we consider the adaptive designs of Section 6. Figure 9 shows the evolution of estimated

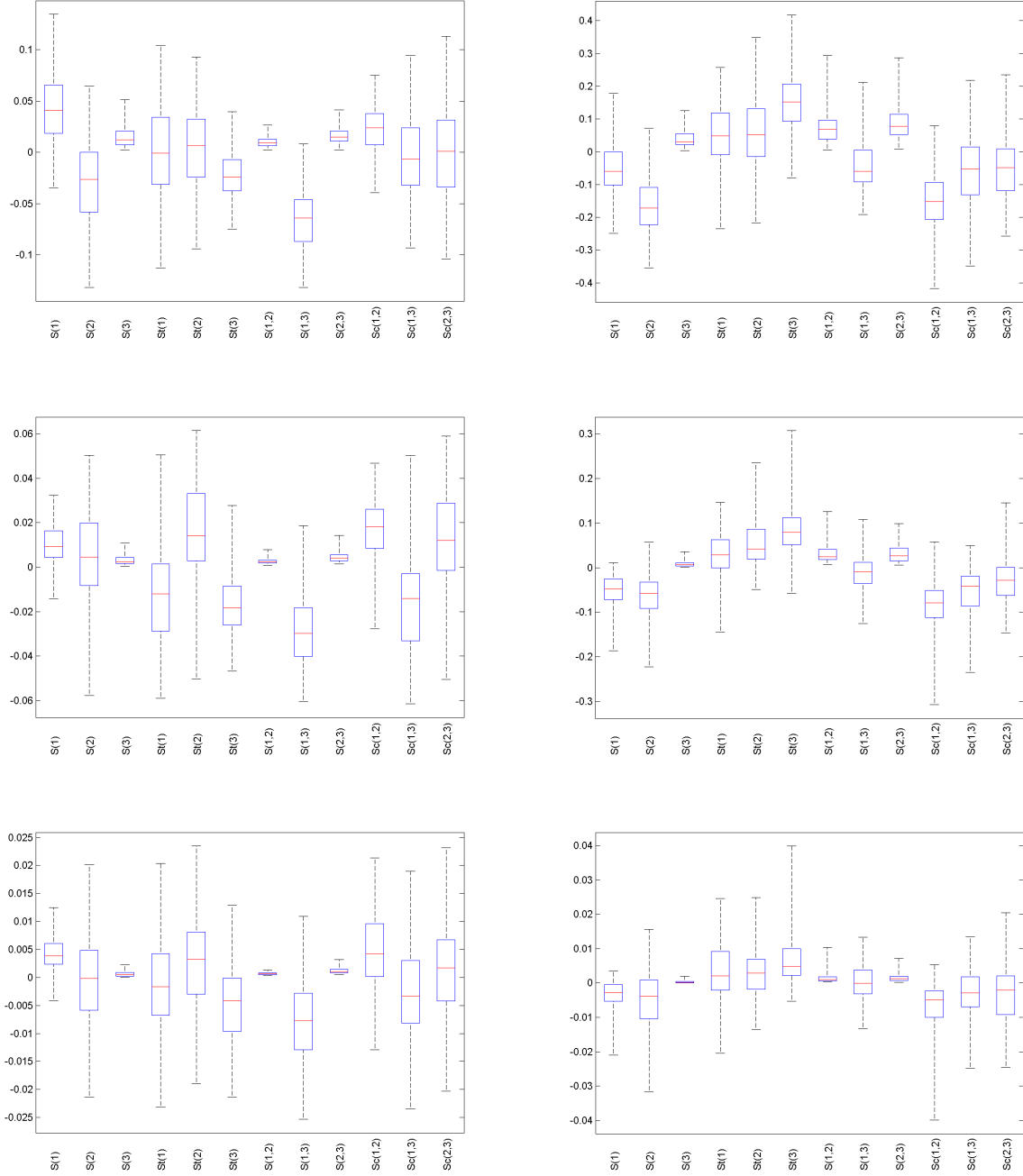


Figure 7: Ishigami function: box-plots of estimation errors of first-order, total, second-order and closed-second-order indices for 100 random Lh designs with $n = 64$ (top), $n = 128$ (middle), $n = 256$ (bottom). Left column: tensorised BLM; right-column: polynomial-chaos model with $D = 5$ (top), $D = 6$, (middle) and $D = 8$ (bottom).

first-order indices \hat{S}_1^n for the tensorised BLM, like in Figure 6, but when the design points \mathbf{x}_n for $n = 11, \dots, 256$ are obtained from (6.4) with \mathcal{X}_Q formed by the first 1,024 points of Sobol' sequence. We observe that convergence to the true values (solid lines) is faster than with the first 256 points

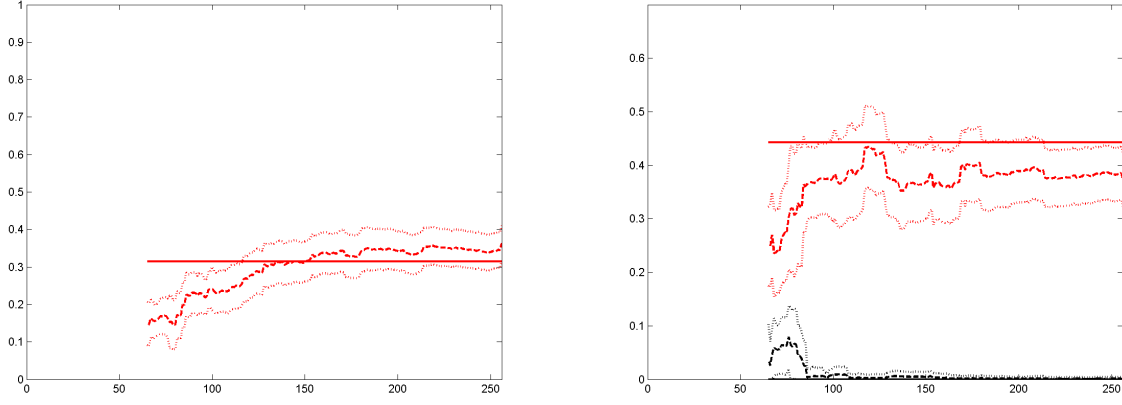


Figure 8: Ishigami function: estimated first-order indices (dashed line) and normal approximation of 95% confidence intervals (dotted lines) with a polynomial-chaos model of total degree $D = 5$; the solid line indicates the true value. Left: S_1 ; right: S_2 (top) and S_3 (bottom).

of Sobol' sequence used in Figure 6. Figure 10-left shows the evolution of variances (5.6) (used to build the 95% credible intervals in Figure 9); on Figure 10-right the design points $\mathbf{x}_{11}, \dots, \mathbf{x}_{256}$ are obtained from (6.2).

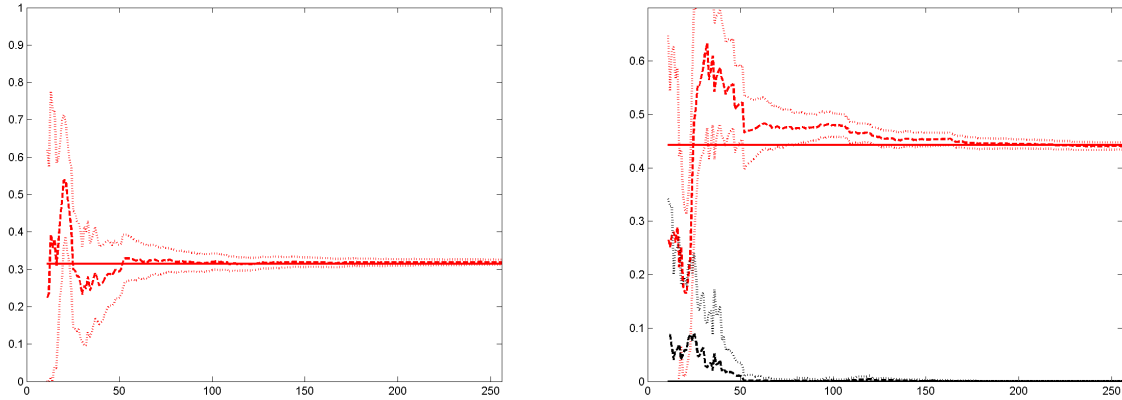


Figure 9: Ishigami function: estimated first-order indices (dashed line) and normal approximation of 95% credible intervals (dotted lines) with a tensorised BLM using $K_{3/2}(x, y; 2)$, $N = 256$, and design points given by (6.4); the solid line indicates the true value. Left: S_1 ; right: S_2 (top) and S_3 (bottom).

7.2 Sobol' g-function

The function is given by $f(\mathbf{x}) = \prod_{i=1}^d f_i(x_i)$ with $f_i(x) = (|4x - 2| + a_i)/(a_i + 1)$ for all i and \mathbf{x} uniformly distributed in the unit cube $\mathcal{X} = [0, 1]^d$; the number d of input variables is arbitrary.

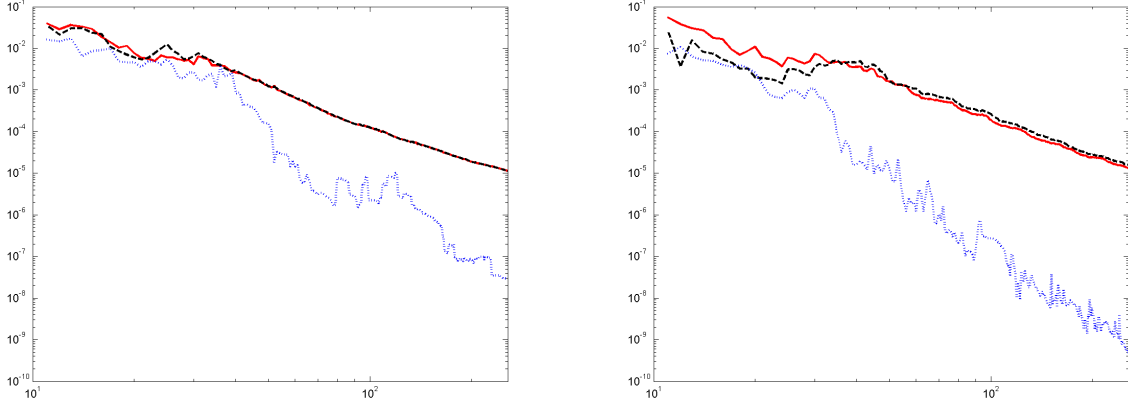


Figure 10: Ishigami function: estimated variances (5.6) of first-order indices S_1 (red solid line), S_2 (black dashed line) and S_3 (blue dotted line) as functions of n , for the design sequences (6.4) (left) and (6.2) (right).

The index corresponding to any index set $\mathcal{U} = \{i_1, i_2, \dots, i_s\} \subseteq \{1, \dots, d\}$ is equal to

$$S_{\mathcal{U}} = \frac{1}{D} \prod_{j=1}^s \frac{1}{3} (a_{i_j} + 1)^{-2},$$

where $D = \prod_{i=1}^d [1 + \frac{1}{3} (a_i + 1)^{-2}] - 1$. We use $a_i = i$ in the example. Note that $f(\cdot)$ is not differentiable. We take $p_i = 0$ for all i and $K_{3/2}(x, y; 2)$ for the construction of the BLM.

Consider first the case $d = 2$. The design space \mathcal{X}_Q is formed by the first 1,024 points of Sobol' sequence. Figure 11-left (respectively, right) shows the adaptive design $\mathbf{x}_{11}, \dots, \mathbf{x}_{128}$ produced by (6.3) for the estimation of first-order indices S_1 and S_2 (respectively, of $S_{1,2}$), when $\mathbf{x}_1, \dots, \mathbf{x}_{10}$ correspond to the first 10 points of Sobol' sequence and $N = 20$ in (4.5). Here, we set $s(\mathbf{x}) = +\infty$ after the evaluation of $f(\mathbf{x})$ to avoid repetitions, see Remark 6.1. The formation of clusters is an indication that N is too small ($N = 20$ whereas $n = 128$). When we do not enforce avoidance of repetitions, we only get 78 (respectively, 53) different design points in Figure 11-left (respectively, right).

Next, using the approach presented in the Appendix, we construct an initial optimal design for the minimisation of the criterion (A.5) with $\varpi = N = 20$. Note that the construction is independent of the function $f(\cdot)$ considered. The ϵ -optimal measure ξ^* ($\epsilon = 10^{-5}$) is supported on 44 points, and Algorithm 1 with $\tau = 1.1$ suggests to remove 26 points from ξ^* , see Figure 12-right. The design ξ_{18} extracted is shown on Figure 12-left, where the disk areas are proportional to the weights w_j of ξ_{18} . Similar behaviours are observed in other situations (with different covariance functions for the BLM, different choices for N and ϖ , estimation of different indices, etc.): the designs obtained are typically well spread over \mathcal{X} , suggesting that the improvement in terms of the precision of the estimation of indices with respect to a more standard space-filling design is doubtful.

Consider finally the case $d = 10$. Figure 13 shows box-plots of the estimation errors $\hat{S}^n - S$ of first-order and total indices obtained for 100 random Lh designs with $n = 512$ points generated as in Section 7.1. The estimation is much more precise with the BLM model (left) than with polynomial-chaos expansion with total degree $D = 3$ (right) — the model has 286 parameters, the model for $D = 4$ would have 1001 parameters. The true value of the indices are given in Table 3, inspection of Figure 13-left indicates that the estimation of first-order and total indices is already reasonably

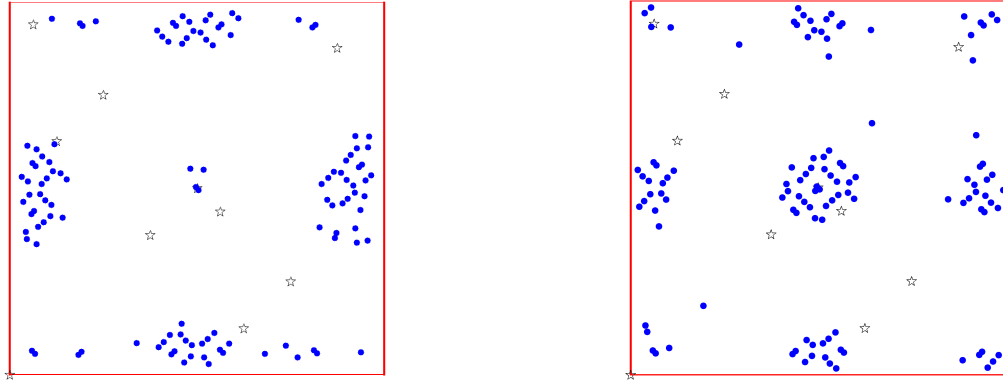


Figure 11: Adaptive designs (dots) constructed with (6.3) (without repetitions, see Remark 6.1) for the estimation of S_1 and S_2 (left) and $S_{1,2}$ (right) in Example 7.2 with $d = 2$; $n = 128$, the first 10 points (stars) correspond to Sobol' sequence.

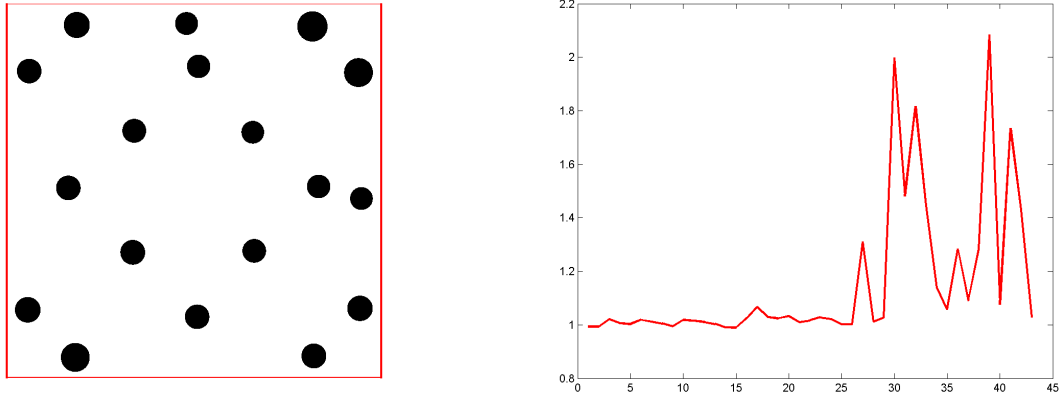


Figure 12: Exact design (18 points) produced by the method in the Appendix for the estimation of first-order indices in Example 7.2 with $d = 2$ and $\varpi = N = 20$. Left: design extracted from the ϵ -optimal design measure ξ^* ($\epsilon = 10^{-5}$); ξ^* has $s^* = 44$ support points (not shown), the disk areas are proportional to the weights w_j of ξ_{18} . Right: evolution of ρ_{s^*-k} as a function of k (see line 5 of Algorithm 1).

accurate for $n = 512$ when using the BLM model (although we only have $\rho(\theta) \simeq 0.6130$ for $\theta = 2$, see (4.7), and although $\mathbf{f}(\cdot)$ is not differentiable). The empirical coverage probabilities, computed as in Section 7.1, are at least 99% for all first-order and total indices.

8 Conclusions and further developments

A metamodeling approach has been proposed for the estimation of Sobol' indices. It relies on Karhunen-Loève expansions and combines the flexibility provided by Gaussian-process models with the easy calculations offered by models based on families of orthonormal functions. The computational cost is moderate (it mainly corresponds to the diagonalisation of a few matrices of limited

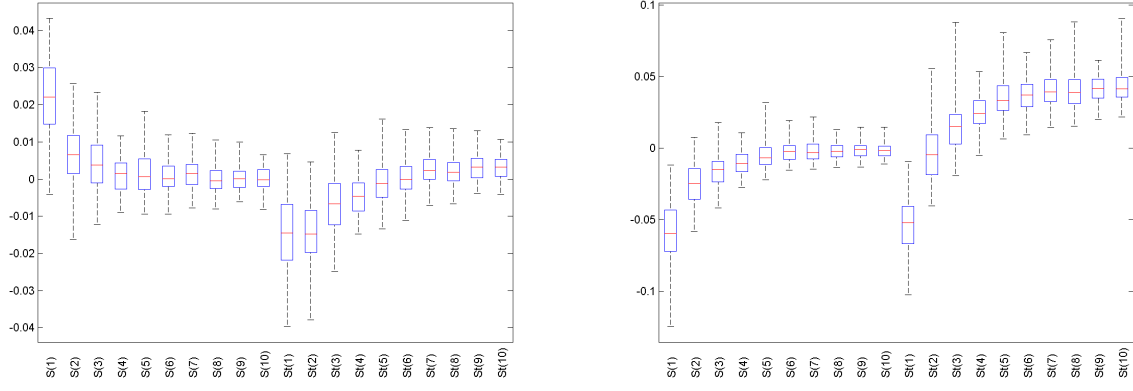


Figure 13: Sobol' g-function for $d = 10$ and $n = 512$: box-plots of estimation errors of first-order and total indices for 100 random Lh designs. Left: tensorised BLM with $K_{3/2}(x, y; 2)$, $p_i = 0$ for all i and $N = n$ in (4.5); right: polynomial-chaos model with total degree $D = 3$.

i	1	2	3	4	5	6	7	8	9	10
S_i	0.4183	0.1859	0.1046	0.0669	0.0465	0.0342	0.0261	0.0207	0.0167	0.0138
\bar{S}_i	0.4631	0.2150	0.1229	0.0792	0.0552	0.0407	0.0312	0.0247	0.0200	0.0165

Table 3: First-order and total indices for Sobol' g-function with $d = 10$ and $a_i = i$ for all i .

dimension), and a normal approximation of the posterior distribution of indices is readily available. It can be used to construct experiments adapted to the estimation of Sobol' indices, and various approaches can be considered: sequential, batch sequential, construction of an initial design.

Several points deserve further investigations. The examples shown indicate that the method is efficient for estimating the indices accurately from a moderate number n of function evaluations, but we have not investigated its convergence properties. Consistent estimation can be obtained by letting N (the number of regression functions in the model) and the q_i (number of points in the one-dimensional quadrature approximations) grow fast enough with n , but we do not know the optimal growth rate. The suboptimal choice made in the paper (q_i constant and $N = n$) could surely be improved, and being able to control the quadrature and truncation errors, under suitable assumptions, would be of major interest. We observed that the inclusion of orthonormal polynomial terms in the model (i.e., taking $p_i \geq 1$) deteriorates the performance of the method. A general confirmation of this phenomenon would be useful, especially as computations are significantly simpler when all p_i equal zero. We have used a unique covariance function with a fixed value of the range parameter θ , with a suggestion for choosing θ in agreement with the projected value of n , see (4.7). The estimation of θ based on function evaluations seems a reasonable alternative; see Remark 4.5 and the example in Section 7.1. It would also be interesting to consider Bayesian Model Averaging, see [18, 29], using a (small) set of T different covariance models $K_i^{(t)}(\cdot, \cdot)$, and possibly different polynomial degrees $p_i^{(t)}$, $t = 1, \dots, T$, in each dimension. Finally, the construction of optimal experiments adjusted to the estimation of Sobol' indices has been considered in Section 6. Adaptive constructions seem promising, in the sense that they provide (slightly) faster convergence of the estimated indices than more usual low-discrepancy sequences. The choice of indices (first or second

order, total, closed. . .) on which adaptive designs should focus remains an open issue. On the other hand, (initial, off-line) optimal designs exhibit a rather classical space-filling property, and therefore do not seem superior to standard uniform designs.

Acknowledgements

This work benefited from several discussions during the SAMO'2016 conference in La Réunion island. The author wishes to thank in particular Bertrand Iooss, Thierry Mara, Elmar Plischke and Bruno Sudret for fruitful exchanges. The author also thanks the two anonymous referees for their careful reading and their insightful comments that helped to improve the presentation.

A Appendix: optimal design

We only consider A-optimal design and minimise $\text{trace}[\mathbf{\Omega}_n(\boldsymbol{\beta}_0)]$ for some $\boldsymbol{\beta}_0$. Direct calculation shows that $\text{trace}[\mathbf{\Omega}_n(\boldsymbol{\beta}_0)]$ is proportional to $\text{trace}[\mathbf{C}(\boldsymbol{\beta}_0)\mathbf{M}_n^{-1}]/(\boldsymbol{\beta}_0^T \mathbf{J} \boldsymbol{\beta}_0)^2$, where

$$\mathbf{C}(\boldsymbol{\beta}) = \sum_{j=1}^J \boldsymbol{\Delta}_{\tilde{\mathbb{L}}_{N,j}}(\boldsymbol{\beta}) \boldsymbol{\beta} \boldsymbol{\beta}^T \boldsymbol{\Delta}_{\tilde{\mathbb{L}}_{N,j}}(\boldsymbol{\beta}), \quad (\text{A.1})$$

and where the $\boldsymbol{\Delta}_{\tilde{\mathbb{L}}_{N,j}}(\boldsymbol{\beta})$ are given by (5.5) (they depend on $\boldsymbol{\beta}$ through the indices $S_{\tilde{\mathbb{L}}_{N,i}}(\boldsymbol{\beta}) = (\boldsymbol{\beta}^T \mathbf{U}_{\tilde{\mathbb{L}}_{N,i}} \boldsymbol{\beta}) / (\boldsymbol{\beta}^T \mathbf{J} \boldsymbol{\beta})$, see (5.3)). Note that $\{\mathbf{C}(\boldsymbol{\beta})\}_{1,1} = 0$.

Consider first batch sequential design, when n_0 evaluations of $\mathbf{f}(\cdot)$ are available and the next n design points \mathcal{D}_n have to be chosen, with $\hat{\boldsymbol{\beta}}^{n_0}$ the current estimated value of $\boldsymbol{\beta}$. We then set $\boldsymbol{\beta}_0 = \hat{\boldsymbol{\beta}}^{n_0}$, substitute \mathbf{M}_{n_0} for $\mathbf{\Lambda}_0^{-1}$ in (5.1), and choose \mathcal{D}_n that minimises $\text{trace}[\mathbf{C}(\hat{\boldsymbol{\beta}}^{n_0})\mathbf{M}_n^{-1}]$. (Note that one may also re-estimate the covariance parameters θ and construct a new BLM based on $\hat{\theta}^{n_0}$.)

For the construction of an initial design (that is, prior to any evaluation of $\mathbf{f}(\cdot)$, when no nominal value $\boldsymbol{\beta}_0$ is available), we suggest to replace each quadratic form in $\boldsymbol{\beta}$ that appears in $\text{trace}[\mathbf{\Omega}_n(\boldsymbol{\beta})]$ by its expectation, with $\boldsymbol{\beta}$ normally distributed $\mathcal{N}(\mathbf{0}, \sigma^2 \mathbf{\Lambda})$. The criterion to be minimised is then $\text{trace}[\tilde{\mathbf{C}}\mathbf{M}_n^{-1}]$, with $\tilde{\mathbf{C}}$ the diagonal matrix

$$\tilde{\mathbf{C}} = \mathbf{\Lambda} \sum_{j=1}^J \boldsymbol{\Delta}_{\tilde{\mathbb{L}}_{N,j}}^2(\tilde{\boldsymbol{\beta}}), \quad (\text{A.2})$$

where $\tilde{\boldsymbol{\beta}} = (\Lambda_{\ell_1}^{1/2}, \dots, \Lambda_{\ell_M}^{1/2})^T$. Note that $\{\tilde{\mathbf{C}}\}_{1,1} = 0$ and $\{\tilde{\mathbf{C}}\}_{k,k} > 0$ for $k \geq 2$ (since $S_{\tilde{\mathbb{L}}_{N,i}}(\tilde{\boldsymbol{\beta}}) > 0$ for all i , so that $\{\boldsymbol{\Delta}_{\tilde{\mathbb{L}}_{N,i}}(\tilde{\boldsymbol{\beta}})\}_{k,k} \neq 0$ for all $k \geq 2$, see (5.5)).

An exchange algorithm for exact design We consider the minimisation of $\text{trace}[\mathbf{C}\mathbf{M}_n^{-1}]$ with respect to \mathcal{D}_n , where $\mathbf{C} = \mathbf{C}(\hat{\boldsymbol{\beta}}^{n_0})$ given by (A.1) in batch sequential design, or $\mathbf{C} = \tilde{\mathbf{C}}$ given by (A.2) in the construction of an initial design, using an exchange-type algorithm, similar to the DETMAX algorithm of [24]. Let $\mathcal{D}_n = \mathcal{D}_n^{(k)}$ denote the current design at iteration k of the algorithm and \mathbf{M}_n denote the corresponding Bayesian information matrix. We suppose that \mathcal{D}_n is such that \mathbf{M}_n is nonsingular. Each iteration comprises two steps. We only consider excursions through $(n+1)$ -point designs, but excursions through designs of size larger than $n+1$ could be considered as well.

First, we consider an optimal design augmentation, obtained by adding a point

$$\mathbf{x}_{n+1} \in \text{Arg max}_{\mathbf{x} \in \mathcal{X}_Q} \frac{\boldsymbol{\psi}^T(\mathbf{x})\mathbf{M}_n^{-1}\mathbf{C}\mathbf{M}_n^{-1}\boldsymbol{\psi}(\mathbf{x})}{s^2(\mathbf{x}) + \boldsymbol{\psi}^T(\mathbf{x})\mathbf{M}_n^{-1}\boldsymbol{\psi}(\mathbf{x})} \quad (\text{A.3})$$

to \mathcal{D}_n , where we set $s^2(\mathbf{x}_i) = +\infty$ for all $\mathbf{x}_i \in \mathcal{D}_n$ to avoid repetitions of observations at the same point. Second, we return to an n -point design by removing a point from $\mathcal{D}_n^+ = \mathcal{D}_n \cup \{\mathbf{x}_{n+1}\}$. Denote by \mathbf{M}_n^+ the Bayesian information matrix corresponding to \mathcal{D}_n^+ . It satisfies

$$(\mathbf{M}_n^+)^{-1} = \mathbf{M}_n^{-1} - \frac{\mathbf{M}_n^{-1}\boldsymbol{\psi}(\mathbf{x}_{n+1})\boldsymbol{\psi}^T(\mathbf{x}_{n+1})\mathbf{M}_n^{-1}}{s^2(\mathbf{x}_{n+1}) + \boldsymbol{\psi}^T(\mathbf{x}_{n+1})\mathbf{M}_n^{-1}\boldsymbol{\psi}(\mathbf{x}_{n+1})},$$

and elementary calculation shows that the optimal choice for a point \mathbf{x}_- to be removed is given by

$$\mathbf{x}_- \in \text{Arg min}_{\mathbf{x} \in \mathcal{D}_n^+} \frac{\boldsymbol{\psi}^T(\mathbf{x})(\mathbf{M}_n^+)^{-1}\mathbf{C}(\mathbf{M}_n^+)^{-1}\boldsymbol{\psi}(\mathbf{x})}{s^2(\mathbf{x}) - \boldsymbol{\psi}^T(\mathbf{x})(\mathbf{M}_n^+)^{-1}\boldsymbol{\psi}(\mathbf{x})}.$$

The design $\mathcal{D}_n^{(k+1)}$ for next iteration is then $\mathcal{D}_n \cup \{\mathbf{x}_{n+1}\} \setminus \{\mathbf{x}_-\}$. The algorithm is stopped when the criterion value does not decrease between two successive iterations, which generally means that $\mathbf{x}_- = \mathbf{x}_{n+1}$. Fedorov's exchange algorithm [11, Chap. 3] could be considered as well, at the expense of heavier computations at each iteration. See also [2, Chap. 12].

Construction of an optimal design measure Let Ξ denote the set of probability measures on \mathcal{X}_Q , a finite subset of \mathcal{X} . Consider the construction of an optimal initial design. For any ξ in Ξ and any $\varpi \in \mathbb{R}^+$, define

$$\mathbf{M}_\varpi(\xi) = \int_{\mathcal{X}_Q} \frac{1}{s^2(\mathbf{x})} \boldsymbol{\psi}(\mathbf{x})\boldsymbol{\psi}^T(\mathbf{x}) d\xi(\mathbf{x}) + \frac{\boldsymbol{\Lambda}_0^{-1}}{\varpi}, \quad (\text{A.4})$$

so that $n\mathbf{M}_n(\mu_n) = \mathbf{M}_n$ given by (5.1) when $\mu_n = (1/n) \sum_{k=1}^n \delta_{\mathbf{x}_i}$ is the empirical measure associated with the design \mathcal{D}_n . An optimal design measure ξ^* is obtained by minimising the L-optimality criterion (L for linear)

$$\mathcal{C}_\varpi(\xi) = \text{trace} [\mathbf{C}\mathbf{M}_\varpi^{-1}(\xi)], \quad (\text{A.5})$$

with $\mathbf{C} = \tilde{\mathbf{C}}$ given by (A.2), with respect to $\xi \in \Xi$. In batch sequential design, we would take $\mathbf{C} = \mathbf{C}(\hat{\boldsymbol{\beta}}^{n_0})$ given by (A.1) for the current estimated value $\hat{\boldsymbol{\beta}}^{n_0}$ and substitute \mathbf{M}_{n_0} for $\boldsymbol{\Lambda}_0^{-1}$ in (A.4). Since \mathcal{X}_Q is finite, the minimisation of $\mathcal{C}_\varpi(\xi)$ forms a finite-dimensional convex optimisation problem, for which many efficient algorithms are available; see, e.g., [28, Chap. 9]. Iteration k of a vertex-direction algorithm transfers some mass to $\mathbf{x}^* \in \mathcal{X}_Q$ that minimises the current directional derivative $F_\varpi(\xi^k, \mathbf{x})$, here given by

$$\begin{aligned} F_\varpi(\xi^k, \mathbf{x}) &= \lim_{\gamma \rightarrow 0^+} \frac{\mathcal{C}_\varpi[(1-\gamma)\xi^k + \gamma\delta_{\mathbf{x}}] - \mathcal{C}_\varpi(\xi^k)}{\gamma} \\ &= -\frac{\boldsymbol{\psi}^T(\mathbf{x})\mathbf{M}_\varpi^{-1}(\xi^k)\mathbf{C}\mathbf{M}_\varpi^{-1}(\xi^k)\boldsymbol{\psi}(\mathbf{x})}{s^2(\mathbf{x})} + \text{trace} \left\{ \mathbf{M}_\varpi^{-1}(\xi^k)[\mathbf{M}_\varpi(\xi^k) - \frac{\boldsymbol{\Lambda}_0^{-1}}{\varpi}]\mathbf{M}_\varpi^{-1}(\xi^k)\mathbf{C} \right\}. \end{aligned}$$

This gives $\mathbf{x}^* \in \text{Arg max}_{\mathbf{x} \in \mathcal{X}_Q} [\boldsymbol{\psi}^T(\mathbf{x})\mathbf{M}_\varpi^{-1}(\xi^k)\mathbf{C}\mathbf{M}_\varpi^{-1}(\xi^k)\boldsymbol{\psi}(\mathbf{x})]/s^2(\mathbf{x})$, compare with (A.3). Note that we have assumed that $\mathbf{M}_\varpi(\xi^k)$ is nonsingular. This can always be achieved through regularisation, by re-introducing a weakly informative prior $\mathcal{N}(\mathbf{0}, \gamma^2 \mathbf{I}_K)$ on the K parameters $\boldsymbol{\alpha}$, with a large γ , so that all diagonal terms of $\boldsymbol{\Lambda}_0^{-1}$ become strictly positive in (A.4), see Section 5.

Extraction of an exact design Let ξ^* denote an ϵ -optimal design measure, satisfying $\min_{\mathbf{x} \in \mathcal{X}_Q} F_{\varpi}(\xi^*, \mathbf{x}) > -\epsilon$, with ϵ a small positive number. The measure ξ^* has a finite number s^* of support points, and can be written as

$$\xi^* = \xi_{s^*} = \sum_{k=1}^{s^*} w_{k:s^*} \delta_{\mathbf{x}_k},$$

where we assume that the weights are ordered by decreasing values: $w_{1:s^*} \geq w_{2:s^*} \geq \dots \geq w_{s^*:s^*}$. Our extraction procedure consists in sequentially reducing the support by transferring the smallest current weight to another support point, suitably chosen (see also Algorithm 1 of [14] for an alternative approach). The size n of the design extracted is not set *a priori*, but is in some sense adapted to the truncation level used to construct the set \mathbb{L}_N , see (4.5). The value of ϖ used to construct ξ^* should be of the same order of magnitude as N , but this choice is not critical. For ξ_s a discrete measure of the form $\xi_s = \sum_{k=1}^s w_k \delta_{\mathbf{x}_k}$, we denote by $\xi_{s,u}$ the uniform measure having the same support; that is, $\xi_{s,u} = (1/s) \sum_{k=1}^s \delta_{\mathbf{x}_k}$. The matrix $s\mathbf{M}_s(\xi_{s,u})$ thus corresponds to the Bayesian information matrix \mathbf{M}_s for the design \mathcal{D}_s formed by the support of ξ_s , see (5.1). The construction is described in Algorithm 1.

Algorithm 1 Greedy algorithm for merging support points

Require: ξ_{s^*} , an ϵ -optimal design measure for $\mathcal{C}_{\varpi}(\cdot)$, a threshold $\tau > 1$;

- 1: set $s = s^*$;
 - 2: **while** $s > 1$ **do**
 - 3: compute $k^* \in \text{Arg max}_{k=1, \dots, s-1} [\psi^T(\mathbf{x}_k) \mathbf{M}_{\varpi}^{-1}(\xi_s) \mathbf{C} \mathbf{M}_{\varpi}^{-1}(\xi_s) \psi(\mathbf{x}_k)] / s^2(\mathbf{x}_k)$;
 - 4: Compute $\xi_{s-1} = \sum_{k=1}^{s-1} w_{k,s} \delta_{\mathbf{x}_k}$ where $w_{k,s} = w_{k:s}$ for $k \neq k^*$ and $w_{k^*,s} = w_{k^*:s} + w_{s:s}$; reorder the weights of ξ_{s-1} by decreasing values, i.e., write $\xi_{s-1} = \sum_{k=1}^{s-1} w_{k:s-1} \delta_{\mathbf{x}_k}$, with $w_{1:s-1} \geq w_{2:s-1} \geq \dots \geq w_{s-1:s-1}$; $s \leftarrow s - 1$;
 - 5: if $\varrho_s = \text{trace}\{\mathbf{C}[s\mathbf{M}_s(\xi_{s,u})]^{-1}\} / \text{trace}\{\mathbf{C}[(s+1)\mathbf{M}_{s+1}([s/(s+1)]\xi_{s+1,u})]^{-1}\} > \tau$, stop;
 - 6: **end while**
 - 7: **return** $n = s + 1$ and \mathcal{D}_n given by the support of ξ_{s+1} .
-

We rescale $\xi_{s+1,u}$ into $[s/(s+1)]\xi_{s+1,u}$ in the test at line 5 of the algorithm, since $\xi_{s+1,u}$ has one more point than $\xi_{s,u}$, so that $\text{trace}\{\mathbf{C}[s\mathbf{M}_s(\xi_{s,u})]^{-1}\} > \text{trace}\{\mathbf{C}[(s+1)\mathbf{M}_{s+1}(\xi_{s+1,u})]^{-1}\}$ for all s , whereas ϱ_s usually fluctuates around 1 in the first steps when s is close to s^* ; see Figure 12-right in Section 7 for an illustration. We can also base the selection of an optimal k^* at line 3 on the comparison between the values of $\mathcal{C}_{\varpi}(\cdot)$, or $\mathcal{C}_s(\cdot)$, achieved for all the $s - 1$ possible mass transfers, at the expense of a significantly larger computational cost when s^* is large.

References

- [1] A. Alexanderian. On spectral methods for variance based sensitivity analysis. *Probability Surveys*, 10:51–68, 2013.
- [2] A.C. Atkinson, A.N. Donev, and R.D. Tobias. *Optimum Experimental Designs, with SAS*. Oxford University Press, 2007.
- [3] G. Blatman and B. Sudret. Efficient computation of global sensitivity indices using sparse polynomial chaos expansions. *Reliability Engineering & System Safety*, 95(11):1216–1229, 2010.
- [4] S. Broda and M.S. Paolella. Evaluating the density of ratios of noncentral quadratic forms in normal variables. *Comput. Statist. Data Anal.*, 53:1264–1270, 2009.

- [5] E. Burnaev, I. Panin, and B. Sudret. Effective design for Sobol indices estimation based on polynomial chaos expansions. In *Symposium on Conformal and Probabilistic Prediction with Applications*, pages 165–184. Springer, 2016.
- [6] R.I. Cukier, C.M. Fortuin, K.E. Shuler, A.G. Petschek, and J.H. Schaibly. Study of the sensitivity of coupled reaction systems to uncertainties in rate coefficients. I Theory. *The Journal of Chemical Physics*, 59(8):3873–3878, 1973.
- [7] R.I. Cukier, J.H. Schaibly, and K.E. Shuler. Study of the sensitivity of coupled reaction systems to uncertainties in rate coefficients. III Analysis of the approximations. *The Journal of Chemical Physics*, 63(3):1140–1149, 1975.
- [8] O. Dubrule. Cross validation of kriging in a unique neighborhood. *Journal of the International Association for Mathematical Geology*, 15(6):687–699, 1983.
- [9] N. Durrande, D. Ginsbourger, O. Roustant, and L. Carraro. Anova kernels and RKHS of zero mean functions for model-based sensitivity analysis. *Journal of Multivariate Analysis*, 115:57–67, 2013.
- [10] B. Efron and C. Stein. The jackknife estimate of variance. *The Annals of Statistics*, 9(3):586–596, 1981.
- [11] V.V. Fedorov. *Theory of Optimal Experiments*. Academic Press, New York, 1972.
- [12] V.V. Fedorov. Design of spatial experiments: model fitting and prediction. In S. Gosh and C.R. Rao, editors, *Handbook of Statistics, vol. 13*, chapter 16, pages 515–553. Elsevier, Amsterdam, 1996.
- [13] J.-C. Fort, T. Klein, A. Lagnoux, and B. Laurent. Estimation of the Sobol indices in a linear functional multidimensional model. *Journal of Statistical Planning and Inference*, 143(9):1590–1605, 2013.
- [14] B. Gauthier and L. Pronzato. Convex relaxation for IMSE optimal design in random field models. *Computational Statistics and Data Analysis*, 113:375–394, 2017.
- [15] L. Gilquin, E. Arnaud, C. Prieur, and H. Monod. Recursive estimation procedure of Sobol’ indices based on replicated designs. 2016. Preprint hal-01291769.
- [16] L. Gilquin, L.A.J. Rugama, E. Arnaud, F.J. Hickernell, H. Monod, and C. Prieur. Iterative construction of replicated designs based on Sobol’ sequences. *Comptes Rendus Mathématique*, 355(1):10–14, 2017.
- [17] D. Ginsbourger, O. Roustant, D. Schuhmacher, N. Durrande, and N. Lenz. On ANOVA decompositions of kernels and Gaussian random field paths. In *Monte Carlo and Quasi-Monte Carlo Methods*, pages 315–330. Springer, 2016.
- [18] J.A. Hoeting, D. Madigan, A.E. Raftery, and C.T. Volinsky. Bayesian model averaging: a tutorial. *Statistical Science*, 14(4):382–417, 1999.
- [19] J.P. Imhof. Computing the distribution of quadratic forms in normal variables. *Biometrika*, 48(3 and 4):419–426, 1961.

- [20] L. Le Gratiet, C. Cannamela, and B. Iooss. A Bayesian approach for global sensitivity analysis of (multifidelity) computer codes. *SIAM/ASA Journal on Uncertainty Quantification*, 2(1):336–363, 2014.
- [21] J. López-Fidalgo, B. Torsney, and R. Ardanuy. MV-optimisation in weighted linear regression. In A.C. Atkinson, L. Pronzato, and H.P. Wynn, editors, *Advances in Model-Oriented Data Analysis and Experimental Design, Proceedings of MODA’5, Marseilles, June 22–26, 1998*, pages 39–50. Physica Verlag, Heidelberg, 1998.
- [22] T.A. Mara and O.R. Joseph. Comparison of some efficient methods to evaluate the main effect of computer model factors. *Journal of Statistical Computation and Simulation*, 78(2):167–178, 2008.
- [23] A. Marrel, B. Iooss, B. Laurent, and O. Roustant. Calculations of Sobol indices for the Gaussian process metamodel. *Reliability Engineering & System Safety*, 94(3):742–751, 2009.
- [24] T.J. Mitchell. An algorithm for the construction of “*D*-optimal” experimental designs. *Technometrics*, 16:203–210, 1974.
- [25] J.E. Oakley and A. O’Hagan. Probabilistic sensitivity analysis of complex models: a Bayesian approach. *Journal of the Royal Statistical Society: Series B (Statistical Methodology)*, 66(3):751–769, 2004.
- [26] C. Prieur and S. Tarantola. Variance-based sensitivity analysis: theory and estimation algorithms. In R. Ghanem, D. Higdon, and H. Owhadi, editors, *Handbook of Uncertainty Quantification*, pages 1–23. Springer, 2016.
- [27] L. Pronzato. Minimax and maximin space-filling designs: some properties and methods for construction. *Journal de la Société Française de Statistique*, 158(1):7–36, 2017.
- [28] L. Pronzato and A. Pázman. *Design of Experiments in Nonlinear Models. Asymptotic Normality, Optimality Criteria and Small-Sample Properties*. Springer, LNS 212, New York, 2013.
- [29] L. Pronzato and M.-J. Rendas. Bayesian local kriging. *Technometrics*, 59(3):293–304, 2017.
- [30] A. Saltelli. Making best use of model evaluations to compute sensitivity indices. *Computer Physics Communications*, 145(2):280–297, 2002.
- [31] A. Saltelli, S. Tarantola, and K.P.-S. Chan. A quantitative model-independent method for global sensitivity analysis of model output. *Technometrics*, 41(1):39–56, 1999.
- [32] J.H. Schaibly and K.E. Shuler. Study of the sensitivity of coupled reaction systems to uncertainties in rate coefficients. II Applications. *The Journal of Chemical Physics*, 59(8):3879–3888, 1973.
- [33] I.M. Sobol’. Sensitivity estimates for nonlinear mathematical models. *Math. Model. Comp. Exp.*, 1(4):407–414, 1993.
- [34] M.L. Stein. *Interpolation of Spatial Data. Some Theory for Kriging*. Springer, Heidelberg, 1999.
- [35] B. Sudret. Global sensitivity analysis using polynomial chaos expansions. *Reliability Engineering & System Safety*, 93(7):964–979, 2008.

- [36] J.-Y. Tissot and C. Prieur. A randomized orthogonal array-based procedure for the estimation of first-and second-order Sobol' indices. *Journal of Statistical Computation and Simulation*, 85(7):1358–1381, 2015.